

New Jersey Institute of Technology Digital Commons @ NJIT

Theses

Theses and Dissertations

Fall 2018

Icing thickness prediction model for overhead transmission lines

Yue Ming

New Jersey Institute of Technology

Follow this and additional works at: <https://digitalcommons.njit.edu/theses>

Part of the [Electrical and Electronics Commons](#)

Recommended Citation

Ming, Yue, "Icing thickness prediction model for overhead transmission lines" (2018). *Theses*. 1635.
<https://digitalcommons.njit.edu/theses/1635>

This Thesis is brought to you for free and open access by the Theses and Dissertations at Digital Commons @ NJIT. It has been accepted for inclusion in Theses by an authorized administrator of Digital Commons @ NJIT. For more information, please contact digitalcommons@njit.edu.

Copyright Warning & Restrictions

The copyright law of the United States (Title 17, United States Code) governs the making of photocopies or other reproductions of copyrighted material.

Under certain conditions specified in the law, libraries and archives are authorized to furnish a photocopy or other reproduction. One of these specified conditions is that the photocopy or reproduction is not to be “used for any purpose other than private study, scholarship, or research.” If a user makes a request for, or later uses, a photocopy or reproduction for purposes in excess of “fair use” that user may be liable for copyright infringement,

This institution reserves the right to refuse to accept a copying order if, in its judgment, fulfillment of the order would involve violation of copyright law.

Please Note: The author retains the copyright while the New Jersey Institute of Technology reserves the right to distribute this thesis or dissertation

Printing note: If you do not wish to print this page, then select “Pages from: first page # to: last page #” on the print dialog screen

The Van Houten library has removed some of the personal information and all signatures from the approval page and biographical sketches of theses and dissertations in order to protect the identity of NJIT graduates and faculty.

ABSTRACT

ICING THICKNESS PREDICTION MODEL FOR OVERHEAD TRANSMISSION LINES

**by
Yue Ming**

Failures in a large electric power system are often inevitable. Severe weather conditions are one of the main causes of transmission line failures. Using the fault data of transmission lines of Shaanxi Power Grid from 2006 to 2016, in conjunction with meteorological information, this paper analyses the relationship between the temporal-spatial distribution characteristics of meteorological disasters and the fault of transmission lines in Shaanxi Province, China.

In order to analyze the influence of micro-meteorology on ice coating, a grey correlation analysis method is proposed. This thesis calculates the grey relational between ice thickness and micro-meteorological parameters such as ambient temperature, relative humidity, wind speed and precipitation. The results show that the correlation between ambient temperature, wind speed and ice thickness is bigger than others. Based on the results of grey correlation analysis, a Multivariate Grey Model (MGM) and a Back Propagation (BP) neural network prediction model are built based on ice thickness, ambient temperature and wind speed. The prediction results of these two models are verified by the case of ice-coating of Shaanxi power grid. The results show that the prediction errors of the two models are small and satisfy the engineering requirement. Then a realistic case is carried out by using these two models. An icing risk map is drawn according to the results.

**ICING THICKNESS PREDICTION MODEL
FOR OVERHEAD TRANSMISSION LINES**

**by
Yue Ming**

**A Thesis
Submitted to the Faculty of
New Jersey Institute of Technology
in Partial Fulfillment of the Requirements for the Degree of
Master of Computer Engineering in Electrical Engineering**

Department of Electrical and Computer Engineering

December 2018

Copyright © 2018 by Yue Ming

ALL RIGHTS RESERVE

APPROVAL PAGE

**ICING THICKNESS PREDICTION MODEL
FOR OVERHEAD TRANSMISSION LINES**

Yue Ming

Dr. Mengchu Zhou, Thesis Advisor Date
Distinguished Professor of Electrical and Computer Engineering, NJIT

Dr. Qing Gary Liu Date
Assistant Professor of Electrical and Computer Engineering, NJIT

Dr. Lianghua He Date
Professor of Department of Computer Science and Technology, Tongji University
Visiting Scholar of Electrical and Computer Engineering, NJIT

BIOGRAPHICAL SKETCH

Author: Yue Ming

Degree: Master of Science

Date: December 2018

Undergraduate and Graduate Education:

- Master of Science in Computer Engineering,
New Jersey Institute of Technology, Newark, NJ, 2018
- Bachelor of Science in Computer Science,
Xidian University, Xi'an, Shaanxi, P. R. China, 2016

Major: Computer Engineering

This thesis is dedicated to my loved parents for giving me continuous support and encouragement since the beginning of my life and studies.

Also, this thesis is dedicated to all the people who believe in the tremendous influence of computer science.

ACKNOWLEDGMENT

I extremely appreciate my advisor, Prof. Mengchu Zhou's support and guidance. He offered me a personal tutorial once a week for guiding me to solve puzzles and process systematic literature review. Without his patience and insightful criticisms, there is no way that I could have finished this thesis.

My thanks and appreciations also go to Dr. Zhengfeng Ming and Mr. Gou who gave me a solid foundation for research.

Meanwhile, I would like to thank my friends and schoolmates, Ms. Haoyue Liu and Mr. Xiaoyu Lu for their constructive comments and encouragement that helped me in the completion of the thesis.

I am also deeply indebted to all the other tutors and teachers in Electrical and Computer Engineering Department for their kind assistance to me.

TABLE OF CONTENTS

Chapter	Page
1 INTRODUCTION.....	1
1.1 Background Information	1
1.2 The Organization of Thesis	5
2 LITERATURE REVIEW	7
2.1 Weather Damage	7
2.2 Icing Loading	11
3 GREY RELATIONAL ANALYSIS.....	15
3.1 Data Sources and Preprocessing.....	15
3.2 Grey Relational Analysis.....	17
3.3 Data Standardization.....	20
4 BASIS OF MODEL BUILDING.....	21
4.1 Artificial Neural Network.....	21
4.2 Neural network prediction model.....	22
4.3 Grey model.....	25
4.3.1 Multivariate grey model (MGM(1,N)).....	26
5 CASE STUDY.....	28
5.1 Introduction.....	28
5.1.1 Shaanxi Power Grid backbone network structure.....	29
5.1.2 Statistics of power grid failures caused by meteorological disasters.....	30
5.2 Data resource.....	31

TABLE OF CONTENTS
(Continued)

Chapter	Page
5.3 Data Preprocessing.....	31
5.4 Grey Relational Analysis (GRA).....	36
5.5 BP Neural Network Prediction Model.....	37
5.6 Multi-variable Grey Model (MGM).....	44
5.7 Results.....	49
6 CONCLUSIONS.....	57
REFERENCES.....	58

LIST OF TABLES

Table		Page
5.1	Statistics of Fault Classification Overhead Transmission Lines with 110-330kV and Above in Shaanxi Power Grid from 2006 to 2016	33
5.2	Monitor Volume and Unit	34
5.3	Original Data	36
5.4	Processed Data	38
5.5	The Grey Relational Analysis Results	40
5.6	Ice Thickness Data and Micro-meteorological Data of 220 kV Wan-Zi Line .	42
5.7	The Performance of ANN Corresponding to the Different Number of Units ..	44
5.8	Comparison Between Predicted Results and Actual Ice Thickness Data with BP Neural Network	45
5.9	Ice thickness data and micro-meteorological data of the 110 kV Bao-Feng line	47
5.10	Comparison Between Prediction Results and Actual Ice Thickness Data with MGM	50
5.11	The Distribution Chart Color Requirement	52
5.12	Each Section's Risk of Ice-flash of Yi-Han #I	54
5.13	Shaanxi Transmission Line in High-risk Area of Ice-flash	56

LIST OF FIGURES

Figure	Page
1.1 Icing-loading	1
1.2 Transmission towers crumpled by the Great North American Ice Storm of 1998	2
4.1 A Three-layer BP Neural Network Frame	24
5.1 Ice Thickness and Micro-meteorological Data Variation Curve	40
5.2 Flow Chart of Ice Thickness Prediction Using BP Neural Network	41
5.3 Comparison Between Predicted Results and Actual Ice Thickness Data with BP Neural Network	46
5.4 Comparison Between Prediction Results and Actual Ice Thickness Data with MGM	50
5.5 Ice Area Map of Shaanxi Province	53
5.5 Ice Area of Power Line Yi-Han #I	54

LIST OF SYMBOLS

©	Copyright
®	Registered
kg	Kilogram
m/s	Meter per second
mm/h	Millimeter per hour
W/m ²	Watts per square meter

LIST OF DEFINITIONS

Standard	A physical or chemical quantity whose value is known exactly, and is used to calibrate or standardize instruments.
Ice thickness	Ice accretion on power transmission and distribution lines.

CHAPTER 1

INTRODUCTION

1.1 Background Information

Security and stability are the basic requirements of power system operation, but due to the frequent extreme weather events in recent years, the threat of natural disasters that transmission lines are faced with is also increasingly serious. Icing is the most important climatic factor influencing the design, operation reliability, and economical characteristics of transmission lines [1]. The faults caused by icing, such as disconnection, the collapse of tower and flashover seriously affect the safe operation of power system [2]. Therefore, it will be useful to estimate and predict the probably icing thickness on transmission lines for guiding the design of transmission lines and the work of ice-resistant.



Figure 1.1 Icing-loading.

Source: ‘Strong winds and icing of power lines cause power outages in settlements in Burgas region’ Vestikavkaza-news, 27.1.2014.

The icing accidents occur frequently all over the world because of the tiny terrain and microclimate. Especially, China was hit by an exceptionally serious weather with long-

lasting freezing rain and snow in January 2008, which caused the direct economic losses of more than 100 billion Yuan [1, 2]. According to the situation of ice flashover, how to reduce the accidents caused by transmission lines icing and improve the running operational of existing transmission lines has become a very urgent issue. At present, the researchers of all over the world have achieved many theoretical results in the mechanism of transmission line icing [2-3,5-6]. With the icing online monitoring and warning technology, they also developed some monitoring devices to run online [4]. But the monitoring technology of transmission line conductor icing has a lot of shortages in actual running process. Because the shortage of sensors, a lot of simplifications are done in the process of building the conductor icing model, and the influence of the parameters such as temperature of conductor was ignored, which led to the mechanical model of computing icing thickness in accurate and unable to get icing density or type correctly. A power system has installed fixed or movable de-icing devices in the most serious icing areas currently. With the aid of the previous icing monitoring method, the information of de-icing is preliminarily given out and the device started artificial de-icing operation with the power department personnel's participation. The computing error of equivalent icing thickness and the lack of icing density or type make it impossible to realize the real-time intelligent operation between icing monitoring and de-icing action. Hence it is urgent to improve the existing monitoring and prediction technology of transmission lines' ice coating.

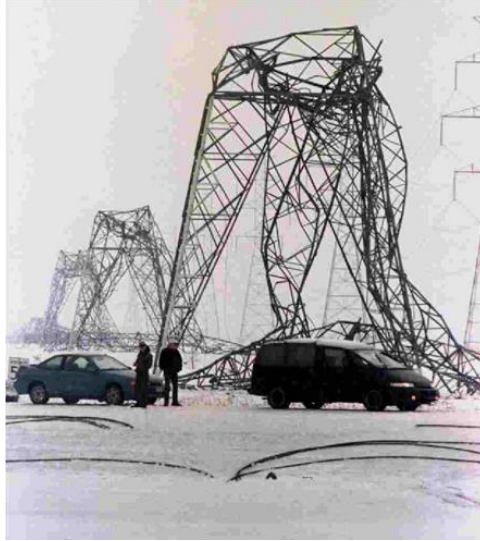


Figure 1.2 Transmission Towers Crumpled by Great North American Ice Storm of 1998
Source: ‘Remember the Ice Storm of ‘98? It was the most devastating and least ferocious of Canadian disasters’ Environment Canada, February 24, 2016.

Climatic loads on overhead power lines induced by atmospheric icing, wind, or ice shedding are the main factors influencing the mechanical design of electrical power systems. Indeed, the icing-load of the transmission lines are underestimated by designers frequently, which leads to the catastrophic damage to systems, excessive repair costs, and extended electrical supply outages. On the other hand, their overestimation drastically increases the installation costs, right-of-way width, and hence, the impact on our environment. In addition, atmospheric icing is a relatively rare, randomly occurring, and difficult-to-forecast meteorological phenomenon. This explains the considerable efforts spent by researchers and designers in two different directions: 1) creation of theoretical (physical) models of icing processes; and 2) statistical analysis of field measurement data records for assessing empirical models for icing processes or forecasting icing loads.

Observation stations are usually built in the area where icing disasters occur frequently. In order to obtain the icing information, such as density, mass, and volume, engineers must cut a portion of ice from the iced transmission line manually, which is very dangerous, and inefficient labor-intensive. Thus, this method cannot be used extensively.

A meteorological model can be applied through a long period of field observations. However, there are many kinds of such models in order to handle the complicated mechanism of an icing phenomenon. In addition, different models often yield different results.

A mechanical model shows the relationship between ice thickness and the load of a transmission line. To calculate ice thickness, such parameters as the sag of a transmission line and load of a tower are needed. In addition, considering that wind load can exert a significant influence on a mechanical model in practice, such model must be modified when wind load takes effect. However, to apply such model, a large amount of field observation data is needed as well. Thus, they are mostly in the theoretical stage.

1.2 The Organization of Thesis

Studying ice thickness calculation and prediction models for overhead transmission lines is important in order to fully understand the ice-covered state of such lines and guide the development of de-icing and ice-melting during the ice-covered time. This research focus on the overhead line ice coating, investigates the ice thickness prediction models. The organization of this thesis is as follows:

Chapter one is the introduction of the topic. This Chapter discusses the background and significance of this topic, and introduces the growth mechanism of over-line ice thickness, and on-line monitoring systems of ice .

Chapter two introduces the research status of the topic of overhead transmission icing monitoring and prediction by given a through literature review.

In the third Chapter, we introduce a new method called Grey Relational Analysis (GRA). Based on the online monitoring of ice and micro-meteorological data preprocessing, the grey relational analysis of ice thickness with respect to such micro-meteorological parameters as ambient temperature, relative humidity, wind speed and rainfall are carried out.

The fourth Chapter studies the ice thickness prediction models by considering micro-meteorology. This chapter proposes two ice thickness prediction models i.e., Multivariate Grey Model (MGM) and Back Propagation (BP) neural network prediction model. The basic theory is introduced.

Chapter five studies two ice thickness prediction models. Based on the pre-processed ice thickness data and micro-meteorological data, the correlation between different micro-meteorological parameters and ice thickness is analyzed. Based on the

results of grey relation analysis, an MGM(1,3) model and a BP neural network prediction model based on ice thickness, ambient temperature and wind speed are established. The prediction effects and application scope of different models are discussed in the actual ice coating case. Then a realistic case study is carried out. An icing risk map is drawn according to the results.

CHAPTER 2

LITERATURE REVIEW

The over-icing of an overhead transmission line poses a serious threat to the safety and stability of a power grid, which may cause a line tripped and damage to hardware facility, and sometimes cause such accidents as power disconnection and tower collapse. Researchers have conducted a large number of theoretical and experimental studies on the ice thickness formation's mechanisms, influencing factors, and online monitoring and prediction of ice thickness.

2.1 Weather-damage

Overhead transmission lines are vital components of a power system. They are also the most vulnerable parts of a power system because they are located outdoors and affected by many factors. Empirical analysis and studies show that overhead transmission lines are highly susceptible to weather, trees, animals, and human factors [7]. Among these factors, severe weather conditions can significantly affect component operation and restoration time in power transmission and distribution systems [8]. Once a power grid disaster occurs, it causes the line to trip in or lead to power failure in a wide range of areas, thus resulting in economic losses.

In any discussion of storm-related power outages, two prominent themes emerge—preparation and recovery. If utility companies are aware of an impending storm or weather-related event that may cause outages, they are expected to prepare for restoration of services in timely a manner. Recovery from any such event depends on the severity of the storm and the resulting damage. However, recovery can be hastened, and the amount of

damage to electric power infrastructure can be minimized, if good maintenance, restoration, organization, and communications strategies are followed on an ongoing basis. Electric utility companies should also be aware of local weather-related events in the past. If an area is prone to seasonal extreme weather, then utility companies would be expected to work with state and local regulatory authorities to look at ways to reduce vulnerabilities of the power and its related infrastructure [9]. The work in [10] shows that extreme weather has a significant influence on critical infrastructures and is considered one of the main causes of global wide-area electrical disturbances. The trend of the annual impact of weather-related blackouts shows that their frequency increased over the last 30 years, with a dramatic increase in the 2000s. In fact, severe weather caused approximately 80% of the large-scale blackouts from 2003 to 2012 [11]. By analyzing the fault data of South African power transmission systems over a 16-period year, the authors in [12] conclude that bird streamers, lightning, fire and pollution are the main causes of South African power system failure. According to the fault reports of the Colombian power transmission system provided in [13], the lightning-caused flashover is as high as 57.6 % of total failures. By comparing the outage rates and outage durations between adverse weather and normal weather, the work [14] concludes that the blackout rate in severe weather conditions are approximately 50% higher than that in normal weather, and the power outage duration during adverse weather conditions are 250% of that under normal weather conditions.

Considering the transmission lines of most areas can be affected by various meteorological and environmental factors in different seasons, the authors [15] propose a method to calculate the time-varying failure rate of transmission lines in a monthly time scale to reflect the time-dependent regulation of transmission line faults. A disaster zone

importance index (DZII) is proposed in [16] to quantify the impact of disasters in different areas on the reliability of a power system, and the influence of different geographical distribution of natural disasters on power system reliability is verified on a real power system. The work in [17] find that climate change (especially severe weather affecting transmission lines such as extreme wind and ice) has a significant impact on transmission line reliability. It is also pointed out that both future climate models and historical climate data should be considered when evaluating the design load specifications for existing or new lines.

The studies have revealed the relationship between transmission line faults and the temporal-spatial distribution characteristics of meteorological disasters by model simulation. Obviously, the severe meteorological conditions can seriously affect overhead transmission lines worldwide. Therefore, it is necessary to determine the regularity of meteorological disasters affecting the stable operation of overhead transmission lines. It helps us to take preventive measures in advance to improve the resilience of a power system. The study on this topic attracts the interest of several researchers [18].

2.2 Ice-loading

The over-icing of an overhead line poses a serious threat to the safety and stability of a power grid, which can cause the line tripped, damage to the hardware, and even the accidents such as disconnection and tower collapse. Researchers have conducted many theoretical and experimental studies on the mechanism, influencing factors, online monitoring and prediction of ice coating on transmission lines.

Currently, the researchers have studied the ice generation and growth mechanism based on thermodynamics and fluid mechanics theory, and proposed different kinds of ice

growth models. At present, typical ice thickness growth prediction models are Imai model, Makkonen thermal equilibrium model and numerical analysis model. The Imai model [19] assumes that wire icing is wet-grown ice, i.e., there is always a thin layer of water on the surface of the wire, and the growth rate per unit length of ice is inversely proportional to the temperature, regardless of the amount of precipitation. The Makkonen heat balance model divides an ice production and growth process into three parts: supercooled droplet collision, capture and freezing [20]. The ice growth parameter is analyzed by establishing a heat balance equation. This model lays a theoretical foundation for the subsequent research on ice growth and melting ice technology. Based on the improvement of the previous model, a new comprehensive numerical model is proposed by Makkonen to study an icicle growth process in detail. This model shows that under the certain conditions, the early model underestimates the ice load of wires. Makkonen indicates that it is easier to form the icing on a power transmission line when the temperature is close to 0°C than the lower temperature.

Other researchers have conducted in-depth theoretical and experimental research of ice production, influencing factors and prediction by establishing test sites, installing test wires and doing simulation experiment in artificial climate chambers [21]. G. Poots and other researchers have studied the torsion of ice-covered conductors with limited span and limited torsional stiffness. They point out the effect of overhead conductor torsion on ice loading. They have further considered the snow surface rate, lift, resistance and other parameters to simulate the shape of an ice surface. The simulated ice shape is consistent with the natural ice shape observed in the field. Farzaneh et al. from Canada have collected and analyzed the ice-covered data and micro-meteorological monitoring data of several

years from the test routes in Quebec. They have explained the relationship between ice coating and micro-meteorology and established a regression model between ice growth rate and micro-meteorological parameters. Meanwhile, the researchers have verified the reliability of this regression model for the test line ice coating prediction. A research institute in Japan has carried out a wind tunnel test to monitor the temperature, humidity, wind speed, snowflake component and liquid water content in the snow near the wires, and statistically analyzed the influence of each monitoring parameter on wire icing. In [22], based on an ice-covered online monitoring system, a meteorological ice-covered prediction model is studied. Through the statistical analysis of the online monitoring data during the ice-covered period from 2004 to 2005, the following conclusions are drawn: When the meteorological parameters such as temperature, wind direction and liquid water content satisfy the icing conditions, the on-line monitoring tension value confirms that the wire is covered with ice; when any of the above meteorological parameters does not satisfy the icing condition, the on-line monitoring tension value confirms that the wire is not covered with ice. In [23], the theoretical analysis and wind tunnel test of overhead wire anti-icing technology are carried out, and the influencing factors such as wire parameters and meteorological conditions are compared and analyzed.

The universities and research institutes in China have carried out extensive research on the factors affecting overhead line ice coating and ice coating prediction through artificial simulation of ice-covered laboratories or establishment of natural ice-covered test stations. Chongqing University has simulated ice coating test in artificial climate laboratory to monitor the variation of wire ice thickness under different meteorological parameters. The effects of ice coating time and meteorological parameters on ice thickness are

statistically analyzed and discussed the effects of meteorological parameters and wire type on ice thickness. Meanwhile, a heat balance equation is established by using heat balance theory. After the ice disaster of China in 2008, Chongqing University has established a natural ice-covered test station in Mountain Xufeng. The work [24-27] uses the Mountain Xufeng Natural Environment Test Station to carry out research on the calculation of over-line ice thickness and ice prediction. Lu et al., have conducted theoretical and experimental research on ice monitoring and ice melting technology in Hunan Power Grid, and achieved fruitful research results.

In recent years, with the construction of smart grids, provincial/state-level network companies in China have successively established large-scale online monitoring systems for transmission lines. According to the testing principle, an online monitoring method of ice coating is mainly a weighing, wire inclination, image monitoring and analog wire one. The weighing method replaces the ball-end loop of the upper part of the insulator with a tension tilt sensor. Then it measures the tensile force of an insulator string, the inclination angle of a line direction, and the angle between a wind plane and vertical plane, thereby calculating the wire coating weight or the equivalent ice thickness of the wire under an ice-covered condition. Xi'an Jinyuan Electric Co., Ltd. and Xi'an University of Engineering have purposed an on-line ice monitoring device [28, 29] with an electronic tension sensor and dual-axis tilt sensor as its core components. It can be used for measuring the wire icing load in the vertical pitch of a linear tower and insulating the wind yaw angle. Then they use these data to calculate the equivalent ice thickness on a wire. Since February 2006, the device has been put into operation in the heavy ice area of Shanxi Luzhou Power Supply Company. The device is running well and has repeatedly monitored the line ice-loading

hazards. The wire inclination method measures the inclination angle of a wire by using the inclination sensor installed at the outlet of a wire clamp calculates the horizontal tension of the wire under the ice-covered condition based on the state equation of a transmission line, and then computes equivalent ice thickness on a wire. The Temperature-Inclination Measuring Ball developed by Hangzhou Hikvision Digital Technology CO., LTD can measure the inclination angle and surface temperature of a wire and monitor the wire coating with a wire inclination method [30]. The image monitoring method uses image processing technology to segment a line ice coating image, extracts the ice coating edge, and estimate the thickness of ice coating by comparing the contours of the wire before and after ice coating. In [31], an ice thickness calculation method based on adaptive threshold image segmentation and Hough transform is proposed. The work [32] uses image segmentation and edge detection techniques to process real-time photos from an on-line ice monitoring device of China Southern Power Grid. The wire thickness measurement results are ideal. In order to facilitate the direct measurement of wire thickness on a wire, the analog wire of the same type as the ground wire is erected near the power transmission line, and then the researchers estimate the thickness of the true wire ice by measuring the thickness of the ice on the simulated wire. This kind of method is called an analog wire method. Due to the difference in the micro-meteorological conditions between ground corridor and high-altitude lines, the thickness of the simulated grounding wire is different from that of the real line. The researchers have proposed the idea of erecting the same type of simulated grounding wire on the transmission tower. The sensor measures the weight of the simulated ground wire to calculate the equivalent ice thickness. Zhejiang Electric Power Company, China, and Hangzhou Haikang Thunderbird Company, China, have

jointly developed a real-time monitoring device for ice-covered analog wires. The device consists of analog wires, cylindrical measuring heads and control boxes. The tension sensor installed in the cylindrical measuring head monitors the weight of the analog wire in real time. The weight of a simulated wire is monitored in real-time and the measurement results are transmitted to the control box through the cable to calculate the combined ice load and equivalent ice thickness of a wire [33]. This device has been put into operation in multiple 220 kV and 500 kV transmission lines of Zhejiang Jinhua Power Supply Bureau, China, since 2007 and the operation effect is good.

With many applications of online monitoring systems, a large amount of online monitoring data has been accumulated. The research on ice-influencing factors and ice-covered prediction based on online monitoring data has gradually begun [34]. Wang et al. from South China University of Technology have conducted statistical analysis on the online monitoring of ice-covered data on transmission lines, and concluded that only a long period of low-temperature rain and snow freezing weather can cause ice hazards that seriously threaten line safety. The linear relationship between ice coating quality and ice coating time is highly correlated, and a simple linear model can be considered for line ice warning [35]. Yang from South China University of Technology has used a statistical method to analyze the ice monitoring and micro-meteorological data of online monitoring of ice-covered monitoring terminals in Guizhou Power Grid [46]. He calculates the linearly dependent coefficient between ice thickness and individual factors such as ambient temperature, relative humidity and wind speed. This work finds that the correlation between single influence factors and icing is small or even non-existent, but it also points out that the linear analysis results are inconsistent with the qualitative analysis results [36].

Based on online monitoring data, Xi'an University of Engineering has studied the relationship between wire icing and micro-meteorological parameters and proposed a fuzzy prediction method based on fuzzy theory to predict the thickness of ice coating [37]. Liu has studied the mid-term and long-term prediction model of ice thickness of transmission lines based on a Markov process, and predicted the maximum annual ice thickness of transmission lines [38], which provides the reference data for the pre-planning of the line.

Since 2008, many researchers have conducted many theoretical and experimental studies of transmission line disaster monitoring and overhead line icing and deicing vibration at engineering laboratories and cooperative companies about transmission. In [39], a kind of overhead transmission monitoring system is designed, and the monitoring system is calibrated. The results show that the error between the measured value of wire tension and theoretical value calculated by the sag formula is about 3%, which satisfies the engineering test requirements. The work [40] develops a set of on-line monitoring device for monitoring a transmission line's status. It uses GPRS communication technology to realize remote monitoring of such status and establishes a state display platform based on a Browser/Server architecture. Its practical application is realized. The work [41] expounds the damage form of the ice-covered wire deicing oscillation on a transmission line and proposes the anti-vibration countermeasures for an overhead line. The studies [42] and [43] carry out numerical simulation analysis and simulation test on the vibration and deicing dynamics of ice-covered overhead wires. In [44], the characteristics of de-icing vibration of an overhead line with real ice-covered and equivalent concentrated mass simulated ice coating are compared. The applicability of a concentrated mass method to simulate ice coating used in the experiment of ice-free tension in overhead line is studied.

CHAPTER 3

GREY RELATIONAL ANALYSIS

The icing process of overhead conductors is obviously affected by the micro-meteorology near the corridor. When the micro-meteorology changes drastically, the regularity of the ice-covered thickness sequence changes. At this time, the prediction error of ice-covered thickness which is based on the single ice thickness time series significantly increases. In this Chapter, the grey relational analysis of micro-weather parameters such as ice thickness and ambient temperature, relative humidity, wind speed and wind direction are carried out. Based on this, the ice thickness and micro-meteorological data are considered in order to propose an ice thickness prediction model to improve the accuracy of prediction results.

3.1 Grey Relational Analysis

The linear relational analysis method is used to study the correlation between the thickness of ice on the transmission line and the influencing factors, such as temperature, humidity, wind speed and wind direction. Due to the limited online monitoring data of an ice-covered online monitoring system and limited by the accuracy of a terminal sensor and network transmission, the data of ice coating and micro-meteorological monitoring are missing and inaccurate, and the data grey scale is large. Therefore, the method of grey relational analysis is used to study the influence of different micro-meteorological factors on the ice coating of the line.

3.1.1 Data Sources and Preprocessing

The data used in this chapter for the analysis of ice and micro-meteorological grey correlation and ice thickness prediction are from Shaanxi Provincial Meteorological

Bureau and State Grid Shaanxi Provincial Dispatching Center. The data used mainly include ice thickness data and micro-meteorological data such as ambient temperature, relative humidity, wind speed, wind direction and rainfall.

Due to in stability and limited reliability of an online monitoring device, the original ice-covered online monitoring data uploaded to the main station system inevitably contains data anomalies and data omissions. Because the dimensions of each monitoring quantity are not uniform, the numerical values are quite different and cannot be directly used for data analysis. Appropriate pre-processing of ice-covered monitoring data, eliminating abnormal data, fulling missing data, standardizing different types of monitoring data, eliminating the influence of data dimension, and improving the accuracy of data analysis results are all necessary.

(1) Eliminate abnormal data

It is generally believed that the meteorological conditions for ice-covered transmission lines are that the ambient temperature is less than or equal to 0°C and the relative humidity is greater than or equal to 85%. Under the influence of breeze vibration or unstable airflow, ice coating data with a small equivalent ice thickness (usually less than 2mm) is often monitored without meeting the ice weather conditions. When analyzing the influencing factors of ice coating, it is necessary to eliminate this part of the abnormal data.

(2) Fulling missing data

Due to the meteorological stations of Shaanxi observe ice phenomenon just in a short time, the data collection of some observatories is not complete, and data missing will occur, resulting in partial loss of real-time ice-covered online monitoring data received by the main station system. In order to ensure the integrity and smoothness of monitoring data,

the linear interpolation method is used to complete the missing data, i.e. the online monitoring data of ice coating collected before and after the missing time is linearly interpolated as the data of the missing periods.

(3) Data normalization

An ice-covered monitoring system needs to monitor different types of monitoring such as equivalent ice thickness, ambient temperature, relative humidity, wind speed, and wind direction. Different types of monitoring data have different unit dimensions. In the process of data analysis or data modeling, “numerical errors” may occur, resulting in errors in the analysis results. Therefore, the ice monitoring data needs to be standardized before analysis. Commonly used normalization methods include initial value, mean value and interval value. In this paper, data normalization (interval value [0, 1]) is used to preprocess all the data.

3.1.2 Grey Relational Analysis, GRA

In 1982, Professor Deng proposed grey system theory. Since then, grey system research has developed rapidly and been applied in many fields such as agriculture, environmental protection, petroleum, and biology. It has been utilized to successfully solved many problems in industrial and agricultural production and scientific research [45]. In this thesis, the research on the prediction of ice thickness is mainly based on the application of grey system theory in prediction problems. Grey model is an important part of the grey system theory. Regression analysis and other commonly used data prediction methods usually require many historical statistical data samples for support. For the case of insufficient sample size, the prediction result is poor. The grey prediction model does not

require many statistical data samples and can be modeled and predicted with a small amount of data, which can effectively solve the small sample data prediction problem.

Grey relational analysis is a part of grey system theory, and it is a new method to study the problem of less data and information uncertainty. Its basic idea is to judge the degree of relevance according to the similarity or similarity of the sequence curve geometry. Its purpose is to analyze the main relationship among various factors in the system, find out the most important factors affecting the system, and guide the system analysis and decision making [45].

(1) Grey absolute correlation analysis

Assume that the sequence of system actions Y_i and the sequence of related factors X_j are equal, and their values are:

$$Y_i = (y_i(1), y_i(2), \dots, y_i(n)) \quad (3-1)$$

$$X_j = (x_j(1), x_j(2), \dots, x_j(n)) \quad (3-2)$$

Sequence Y_i^0 and X_j^0 are the reference sequences of the original sequences Y_i and X_j , respectively, defined as:

$$Y_i^0 = (y_i^0(1), y_i^0(2), \dots, y_i^0(n)) = (0, y_i(2) - y_i(1), \dots, y_i(n) - y_i(1)) \quad (3-3)$$

$$X_j^0 = (x_j^0(1), x_j^0(2), \dots, x_j^0(n)) = (0, x_j(2) - x_j(1), \dots, x_j(n) - x_j(1)) \quad (3-4)$$

Hence, the grey absolute correlation degree of Y_i and X_j is:

$$\varepsilon_{ij} = \frac{1 + |s_i| + |s_j|}{1 + |s_i| + |s_j| + |s_i - s_j|} \quad (3-5)$$

where s_i and s_j can be calculated as:

$$|s_i| = \left| \sum_{k=2}^{n-1} y_i^0(k) + \frac{1}{2} y_i^0(n) \right| \quad (3-6)$$

$$|s_j| = \left| \sum_{k=2}^{n-1} x_j^0(k) + \frac{1}{2} x_j^0(n) \right| \quad (3-7)$$

$$|s_i - s_j| = \left| \sum_{k=2}^{n-1} (y_i^0(k) - x_j^0(k)) + \frac{1}{2} (y_i^0(n) - x_j^0(n)) \right| \quad (3-8)$$

(2) Grey relative correlation analysis

Assume that the sequence of system behavior Y_i and the sequence of related factors X_j are of equal length and the initial values of them are not zero. Their values are:

$$Y_i = (y_i(1), y_i(2), \dots, y_i(n)) \quad (3-9)$$

$$X_j = (x_j(1), x_j(2), \dots, x_j(n)) \quad (3-10)$$

The original sequences of Y_i and X_j are:

$$Y_i' = (y_i'(1), y_i'(2), \dots, y_i'(n)) = \left(1, \frac{y_i(2)}{y_i(1)}, \dots, \frac{y_i(n)}{y_i(1)}\right) \quad (3-11)$$

$$X_j' = (x_j'(1), x_j'(2), \dots, x_j'(n)) = \left(1, \frac{x_j(2)}{x_j(1)}, \dots, \frac{x_j(n)}{x_j(1)}\right) \quad (3-12)$$

So, the grey relative correlation between Y_i and X_j is:

$$r_{ij} = \frac{1 + |s_i'| + |s_j'|}{1 + |s_i'| + |s_j'| + |s_i' - s_j'|} \quad (3-13)$$

and

$$|s_i'| = \left| \sum_{k=2}^{n-1} y_i^0(k) + \frac{1}{2} y_i^0(n) \right| \quad (3-14)$$

$$|s_j'| = \left| \sum_{k=2}^{n-1} x_j^0(k) + \frac{1}{2} x_j^0(n) \right| \quad (3-15)$$

$$|s_i' - s_j'| = \left| \sum_{k=2}^{n-1} (y_i^0(k) - x_j^0(k)) + \frac{1}{2} (y_i^0(n) - x_j^0(n)) \right| \quad (3-16)$$

$$Y_i^0 = (y_i^0(1), y_i^0(2), \dots, y_i^0(n)) = (0, y_i^0(2) - y_i^0(1), \dots, y_i^0(n) - y_i^0(1)) \quad (3-17)$$

$$X_j^0 = (x_j^0(1), x_j^0(2), \dots, x_j^0(n)) = (0, x_j^0(2) - x_j^0(1), \dots, x_j^0(n) - x_j^0(1)) \quad (3-18)$$

(3) Grey comprehensive relational grade

Assume that the sequence of system behavior Y_i and the sequence of related factors X_j are of equal length and their initial values are not zero. ε_{ij} and r_{ij} are the grey absolute correlation degree and the grey relative correlation degree, respectively. $\theta \in [0, 1]$. Then the grey comprehensive correlation degree is:

$$\rho_{ij} = \theta\varepsilon_{ij} + (1 - \theta)r_{ij} \quad (3-19)$$

The grey comprehensive correlation degree can reflect the similarity of the shape change between the system behavior sequence Y_i and the related factor sequence X_j . It can also reflect the closeness between the transformation rates of Y_i and X_j with respect to the starting point. It is an important indicator that can more fully describe the close relationship between sequences. In general, we let $\theta = 0.5$.

3.1.3 Data Standardization

Overhead wire icing is mainly affected by ambient temperature, humidity, wind speed, and wind direction. Since the ambient temperature, humidity, wind speed, and wind direction have different units and different degrees of variation, the data is standardized in order to eliminate the influence of the dimension and the size and magnitude of a variable itself on the analysis results.

The data is standardized here by using extreme standardization:

$$X' = \frac{x - X_{\min}}{X_{\max} - X_{\min}} \quad (3-20)$$

where X' represents the standardized data such as ambient temperature, humidity, wind speed, or wind direction, x is the ambient temperature, humidity, wind speed, or wind direction in a certain place, and X_{\max} (X_{\min}) is the maximum (minimum) ambient temperature, humidity, wind speed, or wind direction.

CHAPTER 4

BASIS OF MODEL BUILDING

4.1 Artificial Neural Network

Artificial neural networks (ANNs) are a mathematical model for information processing and exchange by simulating brain nerves. It is a simulation of biological neural network systems. ANN realizes the solution to a problem through training and optimizes it through certain learning methods. The neural network trains the same series of inputs and outputs as samples, and adequately trains the network according to a certain training algorithm, such that the fitting error is minimized. The trained neural network can grasp the regularity principle of the data sequence change, and the trained neural network model can predict the future changes of the data. Neural networks have good self-learning capabilities, nonlinear mapping capabilities, and generalization capabilities [47-52].

The back propagation (BP) neural network algorithm is proposed by Rumelhard and McClelland in 1986. It is a multi-layer feedforward network. It has an input layer, several hidden layers (one or more layers) and an output layer. The layers are fully connected, and there is no interconnection between the neurons in the same layer. BP neural network can learn and store a large number of input and output mapping without knowing the mathematical equation of mapping relationship in advance and has become one of the most widely used neural network models. The theory proves that with the Sigmoid function as its transfer function, a three-layer neural network with an hidden layer can approximate any nonlinear function.

The traditional BPNN frame often consists of input layer, hidden layer, and output layer [14]. It sometimes contains more than one hidden layer; the outputs of each layer are sent directly to each neuron of the next layer [15]; it also may contain a bias neuron that produces constant outputs but receives no inputs. If the frame includes only one hidden layer, it is called one hidden layer or three-layer BP neural network frame, which is shown in Figure 4.1.

In Figure 4.1, $(x_1, x_2, \dots, x_{N1})$ is expressed as the input nodes of the input layer; $(z_1, z_2, \dots, z_{N3})$ is the output nodes of output layer; $(t_1, t_2, \dots, t_{N3})$ is the expected output nodes, $(\Delta_1, \Delta_2, \dots, \Delta_{N3})$ are described as the errors between actual output nodes and anticipated one, $(w_{i1}, w_{i2}, \dots, w_{ih}, w_{N1N2})$ is the connection weight vector between input layer and hidden layer, and $(w_{h1}, w_{h2}, \dots, w_{hj}, w_{N2N3})$ is the one between hidden layer and output layer. The hidden layer uses the sigmoid transfer function (i.e. *tan sig*), and the output layer uses a linear transfer function (i.e. *purelin*).

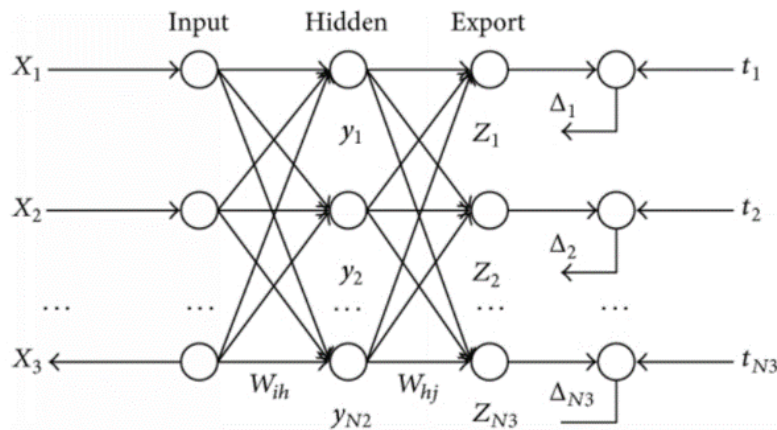


Figure 4.1 A Three-layer BP Neural Network Frame.
 Source: Sen Tian, Jianhong Chen, "An Evaluation Model for Tailings Storage Facilities Using Improved Neural Networks and Fuzzy Mathematics" 2014.

4.2 Neural Network Prediction Model

A BP neural network establishment process uses the error back propagation algorithm, which is a typical supervised learning algorithm. Its main parameters include learning rate, training time, training objectives, transfer function, training function and the number of hidden layer neurons. Each parameter is usually set according to application requirements and experience.

Assuming that the number of nodes in the input layer is m , the nodes of neurons in the hidden layer is l , and the number of nodes in the output layer is n . Then a pair of sample (X, Y) can be represented as $X = [x_1, x_2, \dots, x_m]'$, $Y = [y_1, y_2, \dots, y_n]'$, the set of nodes in hidden layer is $O = [O_1, O_2, \dots, O_l]$.

The weight value matrix between input layer's and hidden layer's nodes W^1 and the weight matrix between hidden layer's and output layer's nodes W^2 are:

$$W^1 = \begin{bmatrix} w_{11}^1 & w_{12}^1 & \cdots & w_{1m}^1 \\ w_{21}^1 & w_{22}^1 & \cdots & w_{2m}^1 \\ \vdots & \vdots & \ddots & \vdots \\ w_{l1}^1 & w_{l2}^1 & \cdots & w_{lm}^1 \end{bmatrix}, \text{ and } W^2 = \begin{bmatrix} w_{11}^2 & w_{12}^2 & \cdots & w_{1n}^2 \\ w_{21}^2 & w_{22}^2 & \cdots & w_{2n}^2 \\ \vdots & \vdots & \ddots & \vdots \\ w_{l1}^2 & w_{l2}^2 & \cdots & w_{ln}^2 \end{bmatrix}$$

The threshold value θ^1 of the nodes in a hidden layer and the threshold value θ^2 of the nodes in an output layer are:

$$\theta^1 = [\theta_1^1, \theta_2^1, \dots, \theta_l^1]' \text{ and } \theta^2 = [\theta_1^2, \theta_2^2, \dots, \theta_n^2]'$$

By using a certain number of example pairs (input and expected output) for training, we have the following steps to establish a neural network model:

- (1) Normalizing the example pairs such that each component falls into $[0, 1]$. A random initial value between $[-1, 1]$ is assigned to weight and threshold.
- (2) The first pair of training example pairs, i.e., the input and expected output, are

selected and substituted into the neural network to calculate the output of the hidden layer and output layer. The output of the j -th node of a hidden layer is:

$$O_j = f\left(\sum_{i=1}^m w_{ji}^1 x_i - \theta_j^1\right) = f(\text{net}_j), j = 1, 2, \dots, l \quad (4-1)$$

where

$$\text{net}_j = \sum_{i=1}^m w_{ji}^1 x_i - \theta_j^1, j = 1, 2, \dots, l \quad (4-2)$$

$f(\bullet)$ is the transfer function of the hidden layer, and usually it is a sigmoid transfer function.

The computed output of an output node is:

$$z_k = g\left(\sum_{j=1}^l w_{kj}^2 O_j - \theta_k^2\right) = g(\text{net}_k), k = 1, 2, \dots, n \quad (4-3)$$

where

$$\text{net}_k = \sum_{j=1}^l w_{kj}^2 O_j - \theta_k^2, k = 1, 2, \dots, n \quad (4-4)$$

$g(\bullet)$ is the transfer function of the output layer, and usually it is a linear transfer function.

- (3) Calculate the error between the neural network output and desired output, and then adjust the weight and threshold values between the layers of the neural network.

The error of an output node is:

$$\begin{aligned} E &= \frac{1}{2} \sum_{k=1}^n (y_k - z_k)^2 = \frac{1}{2} \sum_{k=1}^n \left[y_k - g\left(\sum_{j=1}^l w_{kj}^2 O_j - \theta_k^2\right) \right]^2 \\ &= \frac{1}{2} \sum_{k=1}^n \left\{ y_k - g\left[\sum_{j=1}^l w_{kj}^2 f\left(\sum_{i=1}^m w_{ji}^1 x_i - \theta_j^1\right) - \theta_k^2\right] \right\}^2 \end{aligned} \quad (4-5)$$

The partial derivative of error E with respect to weight W_{kj}^2 between the hidden and output layer nodes is:

$$\frac{\partial E}{\partial w_{kj}^2} = \frac{\partial E}{\partial z_k} \frac{\partial z_k}{\partial w_{kj}^2} = -(y_k - z_k) g'(net_k) O_j = -\delta_k^2 O_j \quad (4-6)$$

where
$$\delta_k^2 = (y_k - z_k) g'(net_k) \quad (4-7)$$

The partial derivative of error E to weight W_{ji}^1 between the hidden and input layer nodes is

$$\frac{\partial E}{\partial w_{ji}^1} = \sum_{k=1}^n \frac{\partial E}{\partial z_k} \frac{\partial z_k}{\partial w_{ji}^1} \frac{\partial O_j}{\partial w_{ji}^1} = -\sum_{k=1}^n (y_k - z_k) g'(net_k) w_{kj}^2 f'(net_j) x_i = -\delta_j^1 x_i \quad (4-8)$$

where
$$\delta_j^1 = \sum_{k=1}^n (y_k - z_k) g'(net_k) w_{kj}^2 f'(net_j) = f'(net_j) \sum_{k=1}^n \delta_k^2 w_{kj}^2 \quad (4-9)$$

Then, we can get the update formula of a weight value:

$$\begin{cases} w_{ji}^1(t+1) = w_{ji}^1(t) + \Delta w_{ji}^1 = w_{ji}^1(t) - \eta^1 \frac{\partial E}{\partial w_{ji}^1} = w_{ji}^1(t) + \eta^1 \delta_j^1 x_i \\ w_{kj}^2(t+1) = w_{kj}^2(t) + \Delta w_{kj}^2 = w_{kj}^2(t) - \eta^2 \frac{\partial E}{\partial w_{kj}^2} = w_{kj}^2(t) + \eta^2 \delta_k^2 O_j \end{cases} \quad (4-10)$$

η^1 and η^2 are the learning rates of the hidden layer and output layer, respectively.

In the same way, the partial derivative of error E to threshold value θ_k^2 between the hidden layer and output layer nodes is

$$\frac{\partial E}{\partial \theta_k^2} = \frac{\partial E}{\partial z_k} \frac{\partial z_k}{\partial \theta_k^2} = -(y_k - z_k) g'(net_k)(-1) = (y_k - z_k) g'(net_k) = \delta_k^2 \quad (4-11)$$

The partial derivative of error E to threshold value θ_j^1 between the hidden layer and output layer nodes is

$$\frac{\partial E}{\partial \theta_j^1} = \sum_{k=1}^n \frac{\partial E}{\partial z_k} \frac{\partial z_k}{\partial O_j^1} \frac{\partial O_j^1}{\partial \theta_j^1} = - \sum_{k=1}^n (y_k - z_k) g'(net_k) w_{kj}^2 f'(net_j)(-1) = \delta_j^1 \quad (4-12)$$

Then, we can get the update formula of the threshold value:

$$\begin{cases} \theta_j^1(t+1) = \theta_j^1(t) + \Delta \theta_j^1 = \theta_j^1(t) - \eta^1 \frac{\partial E}{\partial \theta_j^1} = \theta_j^1(t) - \eta^1 \delta_j^1 \\ \theta_k^2(t+1) = \theta_k^2(t) + \Delta \theta_k^2 = \theta_k^2(t) - \eta^2 \frac{\partial E}{\partial \theta_k^2} = \theta_k^2(t) - \eta^2 \delta_k^2 \end{cases} \quad (4-13)$$

- (4) The next set of examples is selected to be trained on the neural network, and the above two steps are repeated until the global error satisfies some predetermined value, and the learning ends. After all the example sets are used for training, the parameters of the neural network are saved, and a new input vector example is input to the neural network. The neural network output is the predicted value of the input example vector.

4.3 Grey Model

The research on the prediction of ice thickness is mainly based on the application of grey system theory to prediction problems. It is an important part of grey system theory. A grey model does not require many data sets and can be modeled and predicted with a small amount of data, which can effectively solve the small sample data prediction problem.

Grey models predict the future values of a time series based only on a set of the most recent data depending on the window size of the predictor. It is assumed that all data values to be used in grey models are positive, and the sampling frequency of the time series is fixed. From the simplest point of view, grey models to be formulated next can be viewed as curve fitting approaches.

4.3.1 Multivariate Grey Model (MGM(1,N))

The grey prediction model MGM(1, N) expresses a time series in the form of a differential equation. The model MGM(1, N) has high $N - 1$ associated series besides the predicted series. MGM(1, N) is used in this study to forecast the ice thickness. The first index in the MGM(1, N) thus stands for the first order derivative of 1-AGO (Accumulated generating operation) series of the second index (i.e., N variables). The modeling procedures of MGM(1, N) can be carried out as follows. Assume an initial sequence to be

$$x_i^{(0)} = \{x_i^{(0)}(1), x_i^{(0)}(2), \dots, x_i^{(0)}(n)\}, i = 1, 2, \dots, N \quad (4-14)$$

where n is the number of training samples. Then, the first-order accumulated generating operation (1-AGO) of $x_i^{(0)}$, $i = 1, 2, \dots, N$ is defined as:

$$x_i^{(1)} = \{x_i^{(1)}(1), x_i^{(1)}(2), \dots, x_i^{(1)}(n)\}, i = 1, 2, \dots, N \quad (4-15)$$

where

$$x_i^{(1)}(k) = \sum_{m=1}^k x_i^{(0)}(m), i = 1, 2, \dots, N. \quad (4-16)$$

The generated gray model, based on the series $x_i^{(1)}$ is given as the following linear differential equation

$$\frac{dx_1^{(1)}}{dt} + ax_1^{(1)} = b_2x_2^{(1)} + b_3x_3^{(1)} + \dots + b_Nx_N^{(1)} \quad (4-17)$$

where a is the grey developmental coefficient and b_2, b_3, \dots, b_N are the associated coefficients corresponding to associated series respectively. The coefficients a, b_2, b_3, \dots, b_N are the model parameters to be estimated. Equation (4-17) is called the first order grey differential equation and denoted as MGM(1, N) where 1 stands for the first-order derivative of 1-AGO series of x and N stands for N series to have concerns

with the grey differential equation. The values of a and b_2, b_3, \dots, b_N can be estimated via the Ordinary Least Squares (OLS) method as

$$\hat{a} = [a, b_2, b_3, \dots, b_N]^T = (B^T B)^{-1} B^T Y_N \quad (4-18)$$

where

$$B = \begin{bmatrix} -z_1^{(1)}(2) & x_2^{(1)}(2) & \cdots & x_N^{(1)}(2) \\ -z_1^{(1)}(3) & x_2^{(1)}(3) & \cdots & x_N^{(1)}(3) \\ \cdots & \cdots & \cdots & \cdots \\ -z_1^{(1)}(n) & x_2^{(1)}(n) & \cdots & x_N^{(1)}(n) \end{bmatrix} \quad (4-19)$$

$$Y_N = (x_1^{(0)}(2), x_1^{(0)}(3), \dots, x_1^{(0)}(n))^T \quad (4-20)$$

and

$$z^{(1)}(k) = 0.5x^{(1)}(k) + 0.5x^{(1)}(k-1). \quad (4-21)$$

Then, the value of the predicted series obtained by model is as:

$$\hat{x}_1^{(1)}(n+1) = \left[x_1^{(0)} - \frac{1}{a} \sum_{i=2}^N b_i x_i^{(1)}(n+1) \right] e^{-ak} + \frac{1}{a} \sum_{i=2}^N b_i x_i^{(1)}(n+1) \quad (4-22)$$

Applying 1-IAGO (IAGO, Inverse Accumulated Generating Operation) to (4-22), we have the following whitening values:

$$\hat{x}^{(0)}(n+1) = \hat{x}^{(1)}(n+1) - \hat{x}^{(1)}(n). \quad (4-23)$$

CHAPTER 5

CASE STUDY

5.1 Introduction

An overhead transmission line has a harsh operating environment and complex meteorological conditions. It is inevitably subject to the challenges of extreme natural conditions. In the event of a grid disaster, the line may trip, which may also cause power outages in a large area and cause major disasters. Long-term operation experience shows that meteorological disasters such as lightning, wind, ice and snow have a major impact on the transmission network exposed to the external environment, and even lead to the failure of power transmission and transformation equipment, which is one of the main reasons affecting the safety of a power system. Similar statistics from China Power Reliability Management Center show that natural disasters and meteorological factors are the main reasons for the unplanned outage of overhead transmission lines in China's power grid. The 2008 ice disaster caused a large-scale blackout of the power grid. In 2011, the unplanned outage of 220kV-500kV overhead transmission lines caused by natural disasters and meteorological factors accounted for 84.36% of the total number of unplanned outages. Extreme weather disasters such as wind, lightning, and ice disasters can cause multiple transmission line failures in a short period of time, and even cause large-scale power outages.

In order to improve the ability of the Shaanxi power grid system to withstand natural disasters and guarantee that the grid system can operate safely and steadily and provide continuous power supply to important users under natural disaster conditions, the

researchers need to analyze the disasters such as lightning, ice coating, dancing, strong winds and pollution flashes in the Shaanxi province. Shaanxi province is located at the geopolitical center of the China.

Through the analysis of transmission line fault trip accidents in the past ten years, combined with the voltage level of transmission lines, we can determine the high-risk transmission section caused by natural disasters in Shaanxi power grid, and clarify the focus of disaster prevention and reduction of transmission lines in Shaanxi power grid. Based on the historical fault data of the line, we can establish the disaster risk assessment model of the key transmission section of Shaanxi Power Grid. The key sections of the disaster prevention and mitigation of key transmission sections of Shaanxi Power Grid can also be determined. We can carry out the grading risk assessment of key sections of Shaanxi Power Grid and propose the differentiated disaster prevention and mitigation reform plan. Therefore, it is critically important to improve the operational reliability of the power grid in the most economical and reasonable way, the differential disaster prevention and mitigation transformation of the line can maximize the reliable transmission capacity of the power grid under certain disaster levels.

5.1.1 Shaanxi Power Grid Backbone Network Structure

The power transmission system of Shaanxi Province consists of transmission lines, cables, and substation hardware of 110 kV, 330 kV, ± 500 kV, ± 600 kV and 750 kV voltage levels. Among them, there are a total of 217 lines of 330 kV and above, the length is 12614 kilometres and there are 31,326 tower bases. This research is based on the outage data of Shaanxi Province transmission system with 110-330 kV and above from 2006 to 2016. Failures before that period are not taken into consideration since they are not reliable. The

data are obtained from the Shaanxi Provincial Meteorological Bureau and the Shaanxi Provincial Dispatching Centre of the State Grid.

5.1.2 Statistics of Power Grid Failures Caused by Meteorological Disasters

The data of lightning flashover, pollution flashover, icing flashover and windage yaw faults of Shaanxi power grid from 2006 to 2016 are given in Table 5.1.

Table 5.1 Statistics of Fault Classification Overhead Transmission Lines with 110-330kV and Above in Shaanxi Power Grid from 2006 to 2016

Year	Lightning Flashover	Pollution Flashover	Ice Flashover	Windage yaw
2006	10	3	2	2
2007	11	4	2	3
2008	17	2	2	2
2009	12	2	2	3
2010	18	1	1	1
2011	15	0	1	4
2012	16	0	2	2
2013	17	1	1	3
2014	14	1	2	2
2015	18	2	2	3
2016	16	3	2	4
Total	164	19	19	29

Source: Shaanxi Power Grid.

Line icing is a complex physical process in which supercooling water droplets in cloud or fog are captured and frozen by wires, insulators and other structures in a low temperature environment. Ice and snow gather on the insulator, bridge the insulator and provide a conductive path. It can lead to flashover trip and collapse a tower, even cause the

power grid to be paralyzed [4]. Ice-covered disaster is one of the most serious disasters in a power system, especially in high mountain areas [18].

5.2 Data Resource

The basic data used in this project comes from the Shaanxi Provincial Meteorological Bureau and the State Grid Shaanxi Provincial Dispatching Center. There are 100 meteorological stations in Shaanxi Meteorological Bureau. Due to the late construction of some individual stations and lack of their historical data, this study used meteorological data of 32 meteorological stations from 2006 to 2016 for 10 years. The types of meteorological data used are shown in Table 5.2.

Table 5.2 Monitor Volume and Unit

NO.	Monitor Volume	Unit
1	Tension	kg
2	Angle	Degree (°)
3	Temperature	Celsius (°C)
4	Humidity	Percent (%)
5	Wind speed	m/s
6	Wind direction	Degree (°)
7	Precipitation	mm/h
8	Air pressure	Hectopascal (hPa)
9	Sunlight	W/m ²

5.3 Data Pre-processing

Due to the stability and reliability of an online monitoring device, the original ice-covered online monitoring data uploaded to the main station system is inevitably subject to data anomalies and data omissions. At the same time, because the dimensions of each monitoring quantity are not uniform, the numerical values are quite different and cannot be directly used for data analysis. A part of the original data is shown as in Table 5.3. we perform pre-processing of ice-covered monitoring data, i.e., eliminating abnormal data, and complementing missing data, standardizing different types of monitoring data, eliminating the influence of data dimension, to improve the accuracy of data analysis results.

We have introduced the method of data standardization in Chapter 3. We can get the following data after data standardization, shown as Table 5.4. The word “None” in Table 5.4 means that there is no data recorded.

Table 5.3 Original Data

Date	Place	Voltage	r (mm)	L (m)	G (g)	b (mm)	R (mm)
06.1.6	Qian Bin Line	110kV	9	1	None	0	134
06.1.21	Bao-ping,Tuo-shi Line	110kV	9	1	None	0	104
06.1.4	Baoping Line 36#--37#	110kV	9	1	956	11.47	109
07.1.4	Yi-lin Line 105#--106#	110kV	9	None	864	None	119
07.1.4	Bao xian line	110kV	9	None	751	None	129
08.1.8	Bao Feng I、 II	110kV	9	1	None	0	59
09.3.6	Bao Feng I、 II	110kV	9	1	568	7.79	84
11.3.22	Baofeng line II-118#	110kV	9	1	380	5.68	129
11.1.10	Baofeng line I,II-90#--82#	110kV	None	None	None	None	None
12.1.18	Ma han Line 99—102#	330 kV	12	None	None	None	62
12.1.7	Tang Yu Line 1—10#	110kV	7	1	570	8.83	57
13.3.28	Long Ma Line 1#(JB1)	330kV	12	1	2130	17.96	129
14.2.10	An Nan Line I-158#	330kV	12	None	None	None	112
14.1.6	Jin Yi Line 18#---25#	110kV	7	None	None	None	132
15.3.18	820 Line 130#	35kV	9	1	1350	14.63	259
15.1.31	Wan-Zi Line	110kV	7	1	542	8.51	167
16.1.25	Wan-Zi Line	110kV	7	1	542	8.51	167
16.1.31	Wan-Zi Line	110kV	7	1	585	8.90	187
16.3.18	An Nan Line I-158#	330kV	9	None	None	None	134

Source: Shaanxi Power Grid.

*r – Power line's radius; L – Power line's long; G - Ice weight; b – standard ice thickness; R – Power line's radius after ice-loading (with power lines).

Table 5.3 (Continued) Original data

Date	Place	The day-before ice loading				Two days-before ice loading			
		T (°C)	H (%)	R(mm)	W.S.(m/s)	T (°C)	H (%)	R(mm)	W.S.(m/s)
06.1.6	Qian Bin Line	-9°C~-5°C	74	5.3	13.2	-11°C~-4°C	72	5.3	11.8
06.1.21	Bao-ping,Tuo-shi Line	None	None	None	None	None	None	None	None
06.1.4	Baoping Line 36#--37#	-7°C~-3°C	78	6.1	11.6	-8°C~-6°C	77	5.9	12.4
07.1.4	Yi-lin Line 105#--106#	-7°C~-3°C	78	6.1	11.6	-8°C~-6°C	77	5.9	12.4
07.1.4	Bao xian line	-7°C~-3°C	78	6.1	11.6	-8°C~-6°C	77	5.9	12.4
08.1.8	Bao Feng I、 II	None	None	None	None	None	None	None	None
09.3.6	Bao Feng I、 II	None	None	None	None	None	None	None	None
11.3.22	Baofeng line II-118#	None	None	None	None	None	None	None	None
11.1.10	Baofeng line I,II-90#--82#	-5°C~-2°C	81	7.4	9.6	-6°C~-4°C	79	6.8	8.5
12.1.18	Ma han Line 99—102#	-4°C~0°C	77	5.6	8.6	-4°C~-1°C	75	5.5	8.9
12.1.7	Tang Yu Line 1—10#	-6°C~-3°C	83	8.1	11.1	-6°C~-3°C	81	7.9	10.8
13.3.28	Long Ma Line 1#(JB1)	0°C~4°C	72	2.9	8.4	0°C~4°C	74	3.1	8.8
14.2.10	An Nan Line I-158#	0°C~5°C	73	3.1	14.3	-1°C~3°C	71	2.3	13.5
14.1.6	Jin Yi Line 18#---25#	-2°C~3°C	83	3.4	9.1	-2°C~3°C	81	3.3	10.2
15.3.18	820 Line 130#	None	None	None	None	None	None	None	None
15.1.31	Wan-Zi Line	-5°C~-3°C	76	6.2	10.7	-5°C~-2°C	75	6.1	9.7
16.1.25	Wan-Zi Line	-5°C~-2°C	77	6.1	10.9	-5°C~-2°C	78	6.2	11.2
16.1.31	Wan-Zi Line	-5°C~-3°C	76	6.2	10.7	-5°C~-2°C	75	6.1	9.7
16.3.18	An Nan Line I-158#	-1°C~4°C	69	2.1	14.3	-1°C~3°C	71	2.3	13.5

Source: Shaanxi Power Grid.

*T – Ambient temperature; H - Relative humidity; R – Precipitation; W.S. – Wind speed.

Table 5.4 Processed Data

b (mm)	The day of ice-loading				The day-before ice loading				Two days-before ice loading			
	T (°C)	H (%)	R(mm)	W.S. (m/s)	T (°C)	H (%)	R(mm)	W.S. (m/s)	T (°C)	H (%)	R(mm)	W.S.(m/s)
8.5	-7°C	70	4.3	14.3	-8°C	74	5.3	13.2	-11°C~-4°C	72	5.3	11.8
10.5	-5°C	75	5.5	10.5	-5°C	78	6.1	11.6	-8°C~-6°C	77	5.9	12.4
6.5	-5°C	73	4.8	10.9	-5°C	78	6.1	11.6	-8°C~-6°C	77	5.9	12.4
4.2	-5°C	76	5.1	10.6	-6°C	78	6.1	11.6	-8°C~-6°C	77	5.3	12.4
9.1	-4°C	76	6.3	9.9	-5°C	81	7.4	9.6	-6°C~-4°C	79	6.8	8.5
11	-2°C	70	5.0	8.9	-2°C	77	5.6	8.6	-4°C~-1°C	75	5.5	8.9
7.6	-4°C	78	6.6	10.5	-5°C	83	8.1	11.1	-6°C~-3°C	81	7.9	10.8
17.9	2°C	70	2.5	9.4	1°C	72	2.9	8.4	0°C~4°C	74	3.1	8.8
8.2	2°C	69	2.5	15.3	0°C	73	3.1	14.3	-1°C~3°C	71	2.3	13.5
7.6	-1°C	80	3.0	8.8	-1°C	83	3.4	9.1	-2°C~3°C	81	3.3	10.2
7.3	-3°C	72	5.2	9.7	-4°C	76	6.2	10.7	-5°C~-2°C	75	6.1	9.7
6.9	-3°C	75	5.0	9.9	-4°C	77	6.1	10.9	-5°C~-2°C	78	6.2	11.2
7.5	-4°C	74	4.7	10.1	-4°C	76	6.2	10.7	-5°C~-2°C	75	6.1	9.7
10.8	1°C	71	1.5	13.5	0°C	69	2.1	14.3	-1°C~3°C	71	2.3	13.5

Source: Shaanxi Power Grid.

*b – standard ice thickness; T – Ambient temperature; H - Relative humidity; R – Precipitation; W.S. – Wind speed.

5.4 Grey Relational Analysis (GRA)

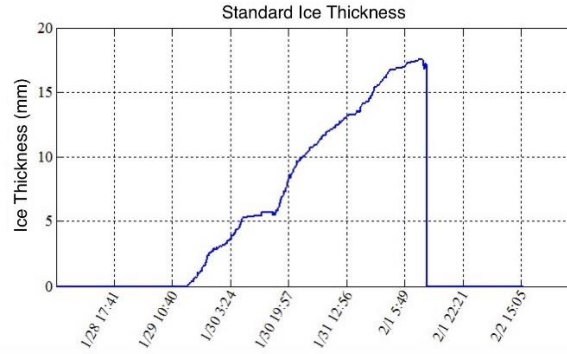
In the previous section, the grey relational analysis is introduced. It is a new method to study the problem related to insufficient data and uncertainty information. The basic idea is to judge the degree of relevance according to the similarity or similarity of the geometrical shape of a sequence curve. The purpose is to analyze the main relationships among the various factors in the system output, to find out the most important factors affecting the system, and to guide the system analysis and decision-making.

In the grey correlation analysis with ice coating and micro-meteorological parameters, the standard ice thickness value is taken as the behavior sequence Y_1 , and the ambient temperature, relative humidity, wind speed and precipitation are taken as the relevant factor sequences X_1, X_2, X_3 , and X_4 .

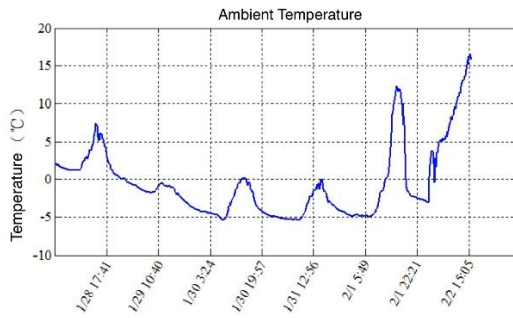
The pre-processed behavior sequence and related factor sequences are substituted into equations (3-1) to (3-11) to calculate the comprehensive correlation between ice thickness and micro-meteorological parameters.

Take the ice thickness and micro-meteorological data from January 25 to February 28, 2015 in Shaanxi Power Grid Wan-Zi line as an example. The data during this time period contains a relatively complete ice-covered cycle. Ice thickness and micro-meteorological data is shown in Figure 5.1.

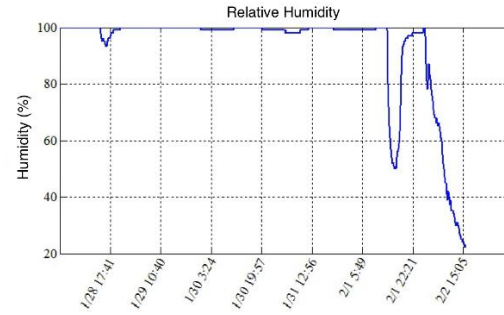
Using the MATLAB software programming calculation, the grey relational analysis results between micro-meteorological factors and ice thickness are obtained, as shown in Table 5.5.



(a) Standard Ice Thickness



(b) Ambient Temperature



(c) Relative Humidity

Figure 5.1 Ice Thickness and Micro-meteorological Data Variation Curve

Table 5.5 The Grey Relational Analysis Results

Micro-meteorological Factors	Temperature	Humidity	Wind speed	Raining
Wan-Zi Line	0.747	0.588	0.682	0.575

It can be seen from the table that there is a certain correlation between temperature, humidity, wind speed and precipitation, and the thickness of ice coating. The correlation between ambient temperature and ice thickness is the largest, followed by wind speed. The precipitation and relative humidity have relatively smaller correlation with ice thickness.

5.5 BP Neural Network Prediction Model

Based on the icing and micro-meteorological data, the flow of ice thickness prediction using a BP neural network is shown in the Figure 5.2.

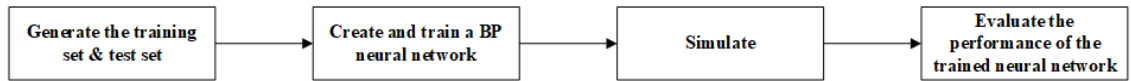


Figure 5.2 Flow Chart of Ice Thickness Prediction Using BP Neural Network

In order to verify the feasibility and effectiveness of the neural network-based prediction model for ice thickness, this work selects the ice thickness data and micro-meteorological data of the 220 kV Wan-Zi line during the ice-covered time in early 2015 as an example, shown as Table 5.6.

The ice-covered and micro-meteorological data with the serial number 1-25 in the table is used as the training set, and the data with the serial number of 26-35 is used as the test set to verify the prediction performance of the neural network-based prediction model.

The training process of the neural network use the rolling training method. For example, the ice thickness data of NO.1-3, with the temperature data and wind speed data of NO. 3 are taken as input set, and the data of NO. 4 is taken as the desired output set, then training this neural network. Until the ice thickness data No. 22-24, with the temperature data and wind speed data of No. 24 are taken as input set, the data with NO. 25 is taken as the expected output, the training process is completed.

Table 5.6 Ice Thickness Data and Micro-meteorological Data of 220 kV Wan-Zi Line

NO.	Date	b (mm)	T (°C)	W.S. (m/s)
1	2015/1/25	0.08	-2.0	0.9
2	2015/1/26	0.32	-2.1	0.8
3	2015/1/27	0.48	-2.2	0.4
4	2015/1/28	0.64	-2.5	0.7
5	2015/1/29	0.80	-2.6	0.2
6	2015/1/30	0.96	-2.6	0.6
7	2015/1/31	1.20	-2.7	1.2
8	2015/2/1	1.36	-3.0	0.2
9	2015/2/2	1.52	-3.2	0.7
10	2015/2/3	1.68	-3.3	0.4
11	2015/2/4	2.00	-3.4	0.3
12	2015/2/5	2.08	-3.4	1.1
13	2015/2/6	2.24	-3.4	0.4
14	2015/2/7	2.32	-3.6	1.3
15	2015/2/8	2.40	-2.1	1.8
16	2015/2/9	2.56	-2.2	2.2
17	2015/2/10	2.80	-2.2	1.4
18	2015/2/11	2.96	-2.3	1.7
19	2015/2/12	3.28	-2.6	1.3
20	2015/2/13	3.44	-2.6	1.3
21	2015/2/14	3.68	-2.7	2.0
22	2015/2/15	3.84	-2.7	1.9
23	2015/2/16	4.00	-2.8	3.2
24	2015/2/17	4.16	-2.9	4.1

NO.	Date	b (mm)	T (°C)	W.S. (m/s)
25	2015/2/18	4.32	-2.9	0.3
26	2015/2/19	4.40	-2.9	0.6
27	2015/2/20	4.56	-3.0	1.2
28	2015/2/21	4.72	-3.1	0.6
29	2015/2/22	4.88	-3.1	0.6
30	2015/2/23	5.12	-2.9	0.5
31	2015/2/24	5.28	-2.7	0.2
32	2015/2/25	5.20	-2.6	0.2
33	2015/2/26	5.28	-2.2	0.2
34	2015/2/27	5.28	-2.6	0.4
35	2015/2/28	5.36	-2.7	0.2

Source: Shaanxi Power Grid

*b – standard ice thickness; T – Ambient temperature; W.S. – Wind speed.

To create a BP neural network, we first to determine its network structure, that is, we need to determine the number of input units, number of hidden layers, number of units in each hidden layer, and number of output units. For this case, the number of input variables is 5 and the output variable is 1. As we show in Chapter 4, a three-layer neural network with a hidden layer can approach an arbitrary nonlinear function. Hence, in this thesis we choose a BP neural network with one hidden layer only. The number of units in the hidden layer has a great influence on the performance of the neural network. If the number is too large, the training time is too long, and the error is increased. If the number is too small, the learning ability of a trained neural network may be too poor. Usually, the number of units is determined based on some empirical formula. We then compare the performance given a different number of units in a network. The number of units with the

best performance is selected to create a neural network. After the neural network structure is determined, parameters such as the training epoch, learning rate, and training target are set, and the training set examples are used to train the network.

Using MATLAB R2012b, we create a three-layer BP neural network. Its transfer function is tansig, activation function is trainlm, learning rate is 0.1, the training target minimum error is 0.00001, and the maximum number of training epoch is 1000. Then we change the number of units in the hidden layer to train a network. The performance of ANN corresponding to the different number of units is shown in Table 5.7. The neural network performance evaluation index uses mean square error (MSE). It is the average squared difference between the estimated values and true values. The smaller MSE, the closer the predicted value is to the true value, and the better neural network performance is.

Table 5.7 The Performance of ANN Corresponding to the Different Number of Nodes in hidden layer

The number of nodes in hidden layer	MSE
3	0.00918
4	0.00667
5	0.01366
6	0.00771
7	0.00910
8	0.00720
9	0.00960
10	0.00547
11	0.00614
12	0.01002

It can be seen from the Table 5.7, MSE is the smallest when the number of nodes in the hidden layer is 10. Hence, we create a three-layer BP neural network with 10 neurons in the hidden layer.

After the training with the NO.1-25 as an example is completed, the ice thickness data of the NO.23-25 with the temperature and wind speed data of NO.25 are taken as inputs set. Then we get a predicated ice thickness value of NO.26. Similarly, we can get the predicted value of NO.26-35. The comparison between the predicted results and the actual ice thickness data is shown in Table 5.8 and Figure 4.4.

Table 5.8 Comparison Between Predicted Results and Actual Ice Thickness Data with BP Neural Network

NO.	Predicted ice thickness (mm)	Actual ice thickness (mm)	Error rate (%)
26	4.48	4.40	1.82
27	4.62	4.56	1.32
28	4.88	4.72	3.39
29	5.04	4.88	3.28
30	5.20	5.12	1.56
31	5.30	5.28	0.38
32	5.32	5.20	2.31
33	5.20	5.28	1.52
34	5.29	5.28	0.19
35	5.37	5.36	0.19

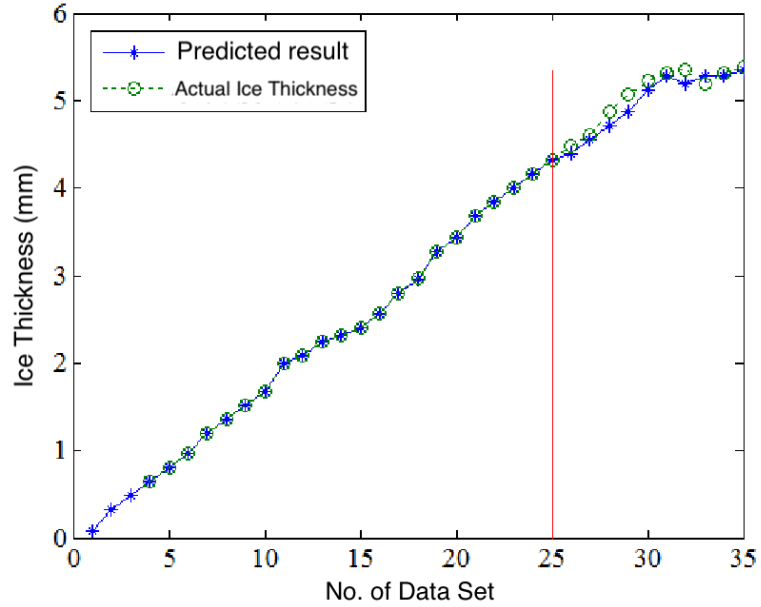


Figure 5.3 Comparison Between Predicted Results and Actual Ice Thickness Data with BP Neural Network.

We can see from Table 5.8 and Figure 5.3, the predicted ice thickness curve is very close to the actual ice thickness curve, and the relative error between the predicted value and the actual value is small. The biggest relative error is 3.39%. It indicates that the neural network prediction model considering micro-meteorology can be applied to the ice thickness prediction to meet the engineering requirements.

5.6 Multi-variable Grey Model (MGM)

The influence of micro-meteorological parameters on the ice thickness of a transmission line is not isolated. Considering the correlation between ice thickness and each micro-meteorological parameter, this work attempts to predict the ice thickness by using Multi-variable Grey Model (MGM). The grey relational analysis between ice thickness and micro-meteorological parameters is carried out in Chapter 3. The result shows that the comprehensive correlation between temperature and ice thickness is the biggest, that

between it and wind speed is second, and that between it and wind direction or relative humidity is small. Therefore, we will consider the ice thickness, temperature, and wind speed to establish an MGM (1, 3) model to predict the ice thickness.

In order to verify the feasibility and effectiveness of MGM(1,3). This paper selects the ice thickness data and micro-meteorological data of the 110 kV Bao-Feng line during the ice-covered time in early 2015 as an example.

Table 5.9 Ice thickness data and micro-meteorological data of the 110 kV Bao-Feng line

NO.	Time	Ice Thickness (mm)	Temperature (°C)	Wind Speed (m/s)
1	2015/1/15	0.24	-1.1	1.6
2	2015/1/16	1.20	-2.5	1.6
3	2015/1/17	2.64	-3.7	0.6
4	2015/1/18	3.04	-4.3	1.6
5	2015/1/19	3.92	-4.5	1.1
6	2015/1/20	5.12	-5.1	0.6
7	2015/1/21	5.36	-3.6	1.2
8	2015/1/22	5.68	-1.5	1.6
9	2015/1/23	5.52	-2.8	1.6
10	2015/1/24	7.04	-3.6	1.2
11	2015/1/25	9.04	-4.6	2.8
12	2015/1/26	10.08	-5.0	2.6
13	2015/1/27	10.96	-5.3	2.0
14	2015/1/28	11.76	-5.3	1.2
15	2015/1/29	12.48	-4.6	2.3
16	2015/1/30	13.12	-1.9	1.5
17	2015/1/31	13.52	-1.4	1.8

NO.	Time	Ice Thickness (mm)	Temperature (°C)	Wind Speed (m/s)
18	2015/2/1	14.24	-3.3	1.6
19	2015/2/2	15.52	-4.2	2.0
20	2015/2/3	16.48	-4.6	1.2
21	2015/2/4	16.88	-4.8	1.3
22	2015/2/5	17.28	-5.0	2.2
23	2015/2/6	17.52	-3.5	1.5

Then we use this data to build an MGM(1,3) model, with the following steps:

- (1) Firstly, we take the data of NO.1-15 to do the 1-AGO (Accumulated generating operation) based on equation (4-14)-(4-17). Then we can get a differential equation of MGM(1,3):

$$\begin{cases} \frac{dx_1^{(1)}}{dt} + b_1 = a_{11}x_1^{(1)} + a_{12}x_2^{(1)} + a_{13}x_3^{(1)} \\ \frac{dx_2^{(1)}}{dt} + b_2 = a_{21}x_1^{(1)} + a_{22}x_2^{(1)} + a_{23}x_3^{(1)} \\ \frac{dx_3^{(1)}}{dt} + b_3 = a_{31}x_1^{(1)} + a_{32}x_2^{(1)} + a_{33}x_3^{(1)} \end{cases} \quad (5-1)$$

- (2) Equation (4-18)-(4-21) are used to calculate \hat{a}_i :

$$\hat{a} = [a, b_2, b_3, b_4]^T = (B^T B)^{-1} B^T Y_N \quad (5-2)$$

where

$$L = \begin{bmatrix} 0.84 & 2.35 & 2.4 & 1 \\ 2.76 & 5.45 & 3.5 & 1 \\ 5.6 & 9.45 & 4.6 & 1 \\ 9.08 & 13.85 & 5.95 & 1 \\ 13.6 & 18.65 & 6.8 & 1 \\ 18.84 & 23 & 7.7 & 1 \\ 24.36 & 25.55 & 9.1 & 1 \\ 29.96 & 27.7 & 10.7 & 1 \\ 36.24 & 30.9 & 12.1 & 1 \\ 44.28 & 35 & 14.1 & 1 \\ 53.84 & 39.8 & 16.8 & 1 \\ 64.36 & 44.95 & 19.1 & 1 \\ 75.72 & 50.25 & 20.7 & 1 \\ 87.84 & 55.2 & 22.45 & 1 \\ 100.64 & 58.45 & 24.35 & 1 \\ 113.96 & 60.1 & 26 & 1 \\ 127.84 & 62.45 & 27.7 & 1 \\ 142.72 & 66.2 & 29.5 & 1 \\ 158.72 & 70.6 & 31.1 & 1 \\ 175.4 & 75.3 & 32.35 & 1 \\ 192.48 & 80.2 & 34.1 & 1 \end{bmatrix}, \quad Y = \begin{bmatrix} 1.2 & 2.5 & 1.6 \\ 2.64 & 3.7 & 0.6 \\ 3.04 & 4.3 & 1.6 \\ 3.92 & 4.5 & 1.1 \\ 5.12 & 5.1 & 0.6 \\ 5.36 & 3.6 & 1.2 \\ 5.68 & 1.5 & 1.6 \\ 5.52 & 2.8 & 1.6 \\ 7.04 & 3.6 & 1.2 \\ 9.04 & 4.6 & 2.8 \\ 10.08 & 5 & 2.6 \\ 10.96 & 5.3 & 2 \\ 11.76 & 5.3 & 1.8 \\ 12.48 & 4.6 & 2.3 \\ 13.12 & 1.9 & 1.5 \\ 13.52 & 1.4 & 1.8 \\ 14.24 & 3.3 & 1.6 \\ 15.52 & 4.2 & 2 \\ 16.48 & 4.6 & 1.2 \\ 16.88 & 4.8 & 1.3 \\ 17.28 & 5 & 2.2 \end{bmatrix}$$

(3) Finally, and the grey forecasting model MGM(1, 3) is established. The ice thickness can be forecasted by using (4-22) and (4-23) in a grey forecasting model MGM(1, 3).

According to the data in Table 5.9, the MGM (1, 3) model is established. We can get predicted ice thickness data of No.16 by using the data of No.1-15 as the input. Similarly, the ice thickness prediction results of No.17-23 can be obtained. The comparison between the prediction results and the actual ice thickness data is shown in Table 5.9 and Figure 5.4.

Table 5.10 Comparison Between Prediction Results and Actual Ice Thickness Data with MGM

NO.	Predicted ice thickness (mm)	Actual ice thickness (mm)	Error rate (%)
16	13.55	13.12	3.28
17	13.92	13.52	2.96
18	13.66	14.24	4.07
19	14.83	15.52	4.45
20	16.09	16.48	2.36
21	17.34	16.88	2.73
22	17.63	17.28	2.03
23	18.30	17.52	4.45

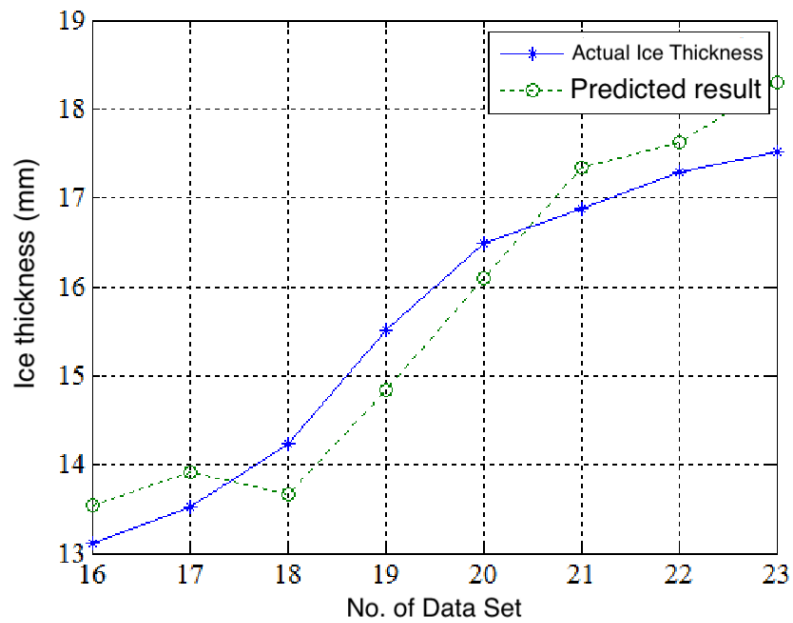


Figure 5.4 Comparison Between Prediction Results and Actual Ice Thickness Data with MGM

It can be seen from Figure 5.4 and Table 5.10 that the predicted ice thickness curve is close to the actual ice thickness curve, and the prediction error is within 5%, which meets the engineering application requirements of the transmission line ice prediction.

5.7 Discuss

Table 5.11 and Table 5.12 shows the performance compared results of BP neural network-based model and MGM (1,3) model. In this case, we use the data from An Nan Line I-158# in early 2015. It contains 63 data set with ice thickness, temperature and wind speed. Then, we use these data test the BPNN model and MGM (1,3) model respectively. We set NO.1-40 data sets as the training set and NO.41-63 data sets as testing set.

Through the above analysis, we can see that the performance of BP neural network-based model is better than the MGM (1,3) in this case.

Table 5.11 Results Comparison of BP Neural Network-based Model and MGM (1,3) Model

NO.	Actual Ice Thickness (mm)	BPNN Model Predicted Results (mm)	MGM (1,3) Model Predicted Results (mm)
41	4.00	4.01	3.03
42	3.84	3.86	2.96
43	3.68	3.67	2.70
44	3.44	3.45	2.45
45	3.28	3.25	2.39
46	2.96	2.92	2.32
47	2.80	2.76	2.01
48	2.56	2.51	1.89
49	2.40	2.37	1.53
50	2.32	2.29	1.48
51	2.24	2.22	1.40
52	2.08	2.01	1.24
53	2.00	1.93	1.00
54	1.68	1.65	0.88
55	1.52	1.55	0.60

56	1.36	1.31	0.42
57	1.20	1.14	0.37
58	0.96	1.01	0.18
59	0.80	0.77	0.13
60	0.64	0.63	0.08
61	0.48	0.45	0.00
62	0.32	0.30	0.00
63	0.08	0.05	0.00

Table 5.11 Running Time Comparison of BP Neural Network-based Model and MGM (1,3) Model






Model	BPNN Model	MGM (1,3)
Running Time (s)	1.76	2.21

5.8 Results

Next, we draw an ice area map based on the results obtained by grey forecasting models. Geographical Information System (GIS) is designed to enable storage, manipulation, analysis and visualization of all types of spatial data. Together with Global Positioning System (GPS) it enables spatial-temporal analysis of extensive data sets that play the key role in integrating big data for various electric power system applications.

The ice thickness prediction result is input into the GIS, and spatial interpolation is performed. Then, according to the obtained 32 meteorological stations' data of the whole Shaanxi province, the ice area map is drawn based on the topographic data, as shown in Figure 5.5. The meaning of colors requirement is shown in Table 5.11.

Table 5.11 The Distribution Chart Color Requirement

Ice Flashover Risk	Ice Thickness (mm)	Legend
Mild	0~5	
	5~10	
Medium	10~15	
	15~20	
Severe	20~30	

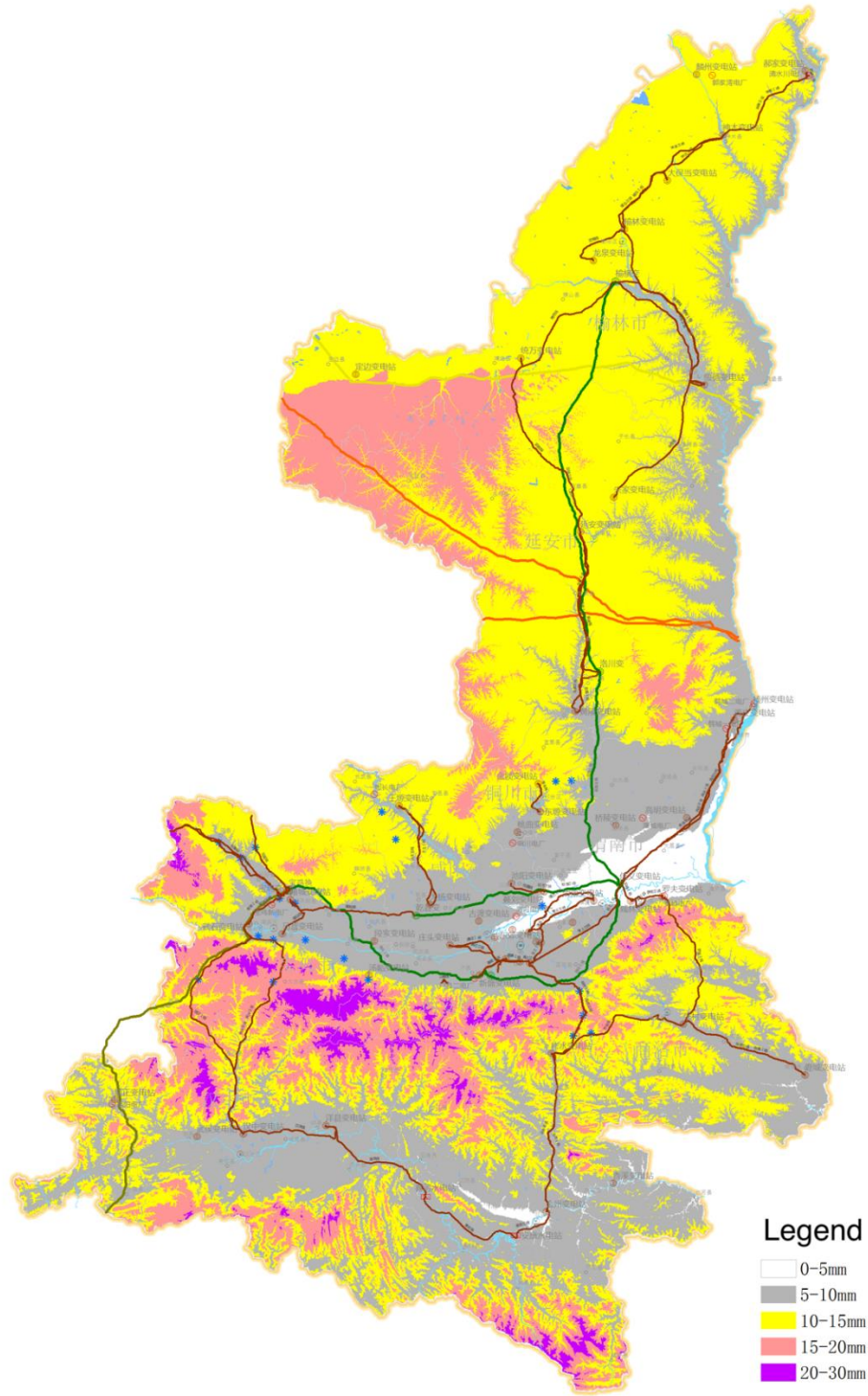


Figure 5.5 Ice Area Map of Shaanxi Province.

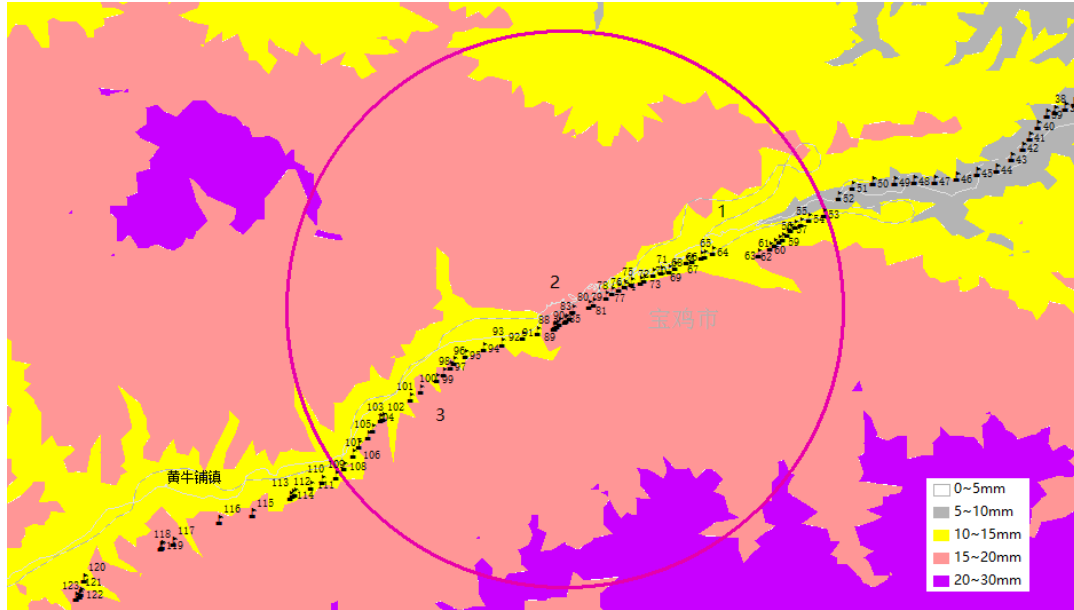


Figure 5.6 Ice Area of Power Line Yi-Han #I.

We put the transmission lines' map and ice area map together and do the spatial overlay analysis. We hope this can effectively guide the relevant agencies and operations to prevent ice disasters and improve work efficiency during the icing time.

Take power line Yi-Han #I as an example. We overlay the transmission lines' map and the ice area map. It is found that some sections of this line have passed through areas with the high ice thickness, as shown in Figure 5.6.

Table 5.12 Each Section's Risk of Ice-flash of Yi-Han #I

Line No.	Tower No.	Ice thickness (mm)	Risk of Ice-flash
1	53~76	10~15	Medium
2	77~90	16~20	Medium
3	91~109	10~15	Medium

It can be seen from Table 5.12 and Figure 5.6, the poles of No.53-76, NO.77-90, and No.91-109 of Yi-Han #I line are in the ice thickness range of 10-15 mm zone, 15-20 mm zone, and 10-15 mm zone, respectively. They all belong to the medium-risk ice area, and the risk of poles No.77-90 is higher than other poles of the transmission line. Therefore, the anti-ice flashing work of different sections of Yi-Han #1 line should be different. Taking the No.77-90 poles as a high-risk ice-covered section that focus on ice disaster prevention, followed by the No.53-76 and No.91-109 poles. The limited manpower, material resources, funds, etc. can thus be allocated according to the degree of risk to better achieve the goal of disaster prevention and mitigation.

Shaanxi Province can be divided into three major natural areas by North Mountain and Qinling Mountain: northern Shaanxi Plateau, Guanzhong Plain and Qinba Mountain Area. The northern Shaanxi Plateau with an elevation of 900 to 1500 meters. The central Guanzhong Plain is formed by the accumulation of the Yellow River, with an altitude of 300 to 800 meters. In the southern Qinba mountainous area, the altitude is 1000 to 3000 meters. Due to the above-mentioned topography, geographical location and climatic characteristics and the influence of the Qinling Mountains, most of ice-covering in Shaanxi province is distributed in the Qinling Mountains, such as the high mountain areas of the Daba Mountain area, and the high altitude and rainfall of the Guanshan area and areas in Gaobei, northern Shaanxi, where the altitude is high, rainfall is heavy, and vegetation is dense.

According to the statistical analysis of the ice grid combined with the ice flash trip, we can determine the high-risk area of ice-flash in Shaanxi province, shown in Table 5.13.

Table 5.13 Shaanxi Transmission Line in High-risk Area of Ice-flash.

Voltage	Transmission Line
330kV	Bao-Mei Line
	Bao-Qin Line
	Yi-Han #I Line
	Ma-Han Line
	Luo-Zhang Line

CHAPTER 6

CONCLUSIONS

This thesis introduces two ice accretion forecasting models based on the BP neural network and gray system theory. Both models are trained, verified, and tested by using an extensive data set containing different icing events which took place over a period of 10 years, in an area of thousands of squared kilometers. The results show the both models can satisfy the engineering requirements.

The grey relational analysis method (GRA) is used to calculate the gray comprehensive correlation between the thickness of ice coating and each micro-meteorological parameter. The correlation between ambient temperature and ice thickness is the largest, followed by wind speed. The precipitation and relative humidity have relatively smaller correlation with ice thickness.

Based on the gray correlation analysis results of ice thickness and micro-meteorological parameters, a multivariate grey model called (MGM(1, 3)) and a BP neural network-based prediction model are built based on two micro-meteorological parameters, i.e., ambient temperature and wind speed. Then we use an actual case in Shaanxi province to verify these two models. The results show that the prediction errors rate of MGM(1,3) and resultant the BP neural network model are all about 5%, which meets the engineering requirements.

Combined the prediction results and geographic information of Shaanxi, China, we use Geographical Information System (GIS) to draw an ice-loading risk map. We hope that this can effectively guide the relevant departments of power companies to prevent ice disasters and improve work efficiency during the icing time.

REFERENCES

- [1] Y. Zhou, A. Pahwa, S. S. Yang, *Modeling weather-related failures of overhead distribution lines*, IEEE Trans. Power Syst. 21(4) (2006) 1683–1690.
- [2] S. S. Halilcevic, F. Gubina A. F. Gubina, *Prediction of power system security levels*, IEEE Trans. Power Syst. 24(1) (2009) 368–77.
- [3] K. Alvehag, L. Soder, *A reliability model for distribution systems incorporating seasonal variations in severe weather*, IEEE Trans. Power Deliv. 26(2) (2011) 910–919.
- [4] M. Panteli, P. Mancarella, *Influence of extreme weather and climate change on the resilience of power systems: impacts and possible mitigation strategies*, Electr. Power Syst. Res. 127 (2015) 259–270.
- [5] A. Kenward, U. Raja, *Blackout: Extreme weather, climate change and power outages*, 2014.
- [6] U.J. Minnaar, C. T. Gaunt, F. Nicolls, *Characterization of power system events on South African transmission power lines*, Electr. Power Syst. Res. 88 (2012) 25–32.
- [7] D. Aranguren, J. González, A. Cruz, J. Inampué, H. Torres, and P. S. Pérez-Tobón, *Lightning strikes on power transmission lines and lightning detection in Colombia*, *International Symposium on Lightning Protection (XIV SIPDA)* (2017) 273–278.
- [8] A. Ozdemir, M. Bagriyanik, A. Kaypmaz, O. Gul, I. Ilisu, *Impact of adverse weather conditions on outage statistics of 154 KV power transmission system*, *International Conference on Electronics, Communications and Computers (CONIELECOMP)* (2015) 29–34.
- [9] J. Wang, X.F. Xiong, N. Zhou, Z. Li, S.J. Weng, *Time-varying failure rate simulation model of transmission lines and its application in power system risk assessment considering seasonal alternating meteorological disasters*, IET Gener. Transm. Distrib. 10(7) (2016) 1582–1588.
- [10] J. Liu, N. Zhang, C. Kang, J.H. Bai, L. Cheng, J. Tan, Z.J. Xie, J.H. Huang, *Geographical impacts of natural disaster on power system reliability*, *IEEE Power Energy Society General Meeting* (2015) 1–5.
- [11] S. N. Rezaei, L. Chouinard, S. Langlois, F. Légeron, *Analysis of the effect of climate change on the reliability of overhead transmission lines*, Sust. Cities Soc. 27 (2016) 137–144.
- [12] R.G. Jiang, J.C. Xie, H.L. He, J.G. Luo, and J.W. Zhu, *Use of four drought indices for evaluating drought characteristics under climate change in Shaanxi, China: 1951–2012*, Natural Hazards 75(3) (2015) 2885–2903.

- [13] Y. Cheng, A. Huo, J. Zhang, Y. Lu, *Early warning of meteorological geohazard in the loess plateau: a study in Huangling County of Shaanxi Province in China*, Environ. Earth Sci. 73(3) (2015) 1057–1065.
- [14] T. Short, *Electric Power Distribution Handbook*, Boca Raton, FL: CRC, 2004.
- [15] R.E. Brown, *Electric Power Distribution Reliability*, CRC, 2009.
- [16] N. Balijepalli, S.S. Venkata, C.W. Richter, R.D. Christie, V.J. Longo, *Distribution system reliability assessment due to lightning storms*, IEEE Trans. Power Deliv. 20(3) (2005) 2153–2159.
- [17] J. A. Morales, E. Orduña, C. Rehtanz, *Classification of lightning stroke on transmission line using multi-resolution analysis and machine learning*, Electr. Power Energy Syst. 58 (2014) 19–31.
- [18] X. B. Meng, L.M. Wang, H. Lei, G.J. Fu, B. Q. Sun, H. Wei, *Dynamic characteristic of ice-shedding on UHV overhead transmission lines*, Cold Reg. Sci. Tech. 66(1) (2011) 44–52.
- [19] M. Darveniza, C. Arnold, P. Blackmore, P. Rainbird, *The relationships between weather variables and reliability indices for a distribution system in South-East Queensland*, 19th International Conference on Electricity Distribution, Vienna (2007) 21-24.
- [20] J. Wang, Y. Tang, J. Shao, M. Long, *A real-time alarm and early warning model for windage yaw of cat-head type tower*, IEEE Trans. Elec. Electron. Eng. 13(2018) 448-454.
- [21] J.B. Yang, F.L. Yang, Q.H. Li, D.J. Fu, Z.F. Zhang, *Dynamic responses analysis and disaster prevention of transmission line under strong wind*, International Conference on Power System Technology (2010) 1–6.
- [22] X.F. Xiong, J. Wang, J. Yuan, N.H. Zhang, *Temporal and spatial environments dependent power grid failure method and its application in power grid reliability assessment*, Power Syst. Prot. Contr. 43(15) (2015) 28–35.
- [23] L. Peter, R. Vajeth, *Strategies for bating environmental influences on overhead lines to improve quality of supply*, IEEE Power Engineering Society Inaugural Conference and Exposition in Africa (2005) 80–87.
- [24] M. T. Gençoğlu, M. Cebeci, *The pollution flashover on high voltage insulators*, Electr. Power Syst. Res. 78(11) (2008) 1914–1921.
- [25] O. E. Gouda, A. Z. El Dein, *Experimental techniques to simulate naturally polluted high voltage transmission line insulators*. IEEE Trans. Dielectr. Electr. Insul. 21(5) (2014) 2199–2205.
- [26] M.S. Banjanin, *Application possibilities of special lightning protection systems of overhead distribution and transmission lines*, Electr. Power Energy Syst. 100 (2018), 482–88.

- [27] Q. Hu, S.J. Wang, H.J. Yang, L.C. Shu, X.L. Jiang, H.T. Li, J.H. Qi, Y.Q. Liu, *Effects of icing degree on ice growth characteristics and flashover performance of 220kV composite insulators*, Cold Reg. Sci. Tech.128 (2016) 47–56.
- [28] Imai. Studies on Ice Accretion [J]. *Researches on Snow and Ice*, 1953, 3(1):35-34.
- [29] Makkonen L. The growth of icicles [R]. *In the Proceedings of the Fourth IWAIS*, 1988:236–242.
- [30] Makkonen L. *A Model of Icicle Growth* [J]. Journal of Glaciology, 1988, 34(116): 64-70.
- [31] MAKKONEN L. *Modeling of ice accretion on wires*[J].Journal of Climate Applied Meteorology, 1984, 23(6):929-939.
- [32] MAKKONEN L, STALLABRASS J R. *Experimentson the cloud droplet collision efficiency of cylinders*[J]. Journal of Climate Applied Meteorology, 1987, 26(10): 1406-1411.
- [33] Makkonen L. The Origin of Spongy Ice [J]. *In the Proceedings of the Tenth IAHR Symposium on Ice*, 1990, 2:1022-1030.
- [34] Makkonen L. Fujii Y. Spacing of Icicles [J]. *Cold Regions Science and Technology*, 1993, 21:317-322.
- [35] Lasse Makkonen. *Modeling power line icing in freezing precipitation*[J]. Atmospheric Research, 1998 (1).
- [36] G. Poots, P.L.I. Skelton. *The effect of aerodynamic torque on the rotation of an overhead line conductor during snow accretion* [J]. Atmospheric Research, 1995 (3).
- [37] G. Poots, P. L.I. Skelton. *Simulation of wet-snow accretion by axial growth on a transmission line conductor* [J]. Applied Mathematical Modelling, 1995 (9).
- [38] Savadjiev K, Farzaneh M. *Modeling of icing and ice shedding on overhead power lines based on statistical analysis of meteorological data* [J]. IEEE Trans on Power Delivery, 2004, 19(2): 715-721.
- [39] Farzaneh M, Savadjiev K. *Statistical analysis of field data for precipitation icing accretion on overhead power lines* [J]. IEEE Trans on Power Delivery, 2005, 20(2):1080-1087.
- [40] Matsushita T, Nishio F. *Local influence on occurrence of freezing rain and precipitation icing in Japan*[C]. 11th International Workshop on Atmospheric Icing of Structures (IWAIS), 2005.
- [41] Veal A, Skea A. *Method of forecasting icing by meteorology model*. 11th International Workshop on Atmospheric Icing of Structures (IWAIS), 2005.
- [42] Peter Z, Farzaneh M, Kiss L I. *Assessment of the current intensity for preventing ice accretion on overhead conductors*[J]. Power Delivery IEEE Transactions on, 2007, 22(1):565 - 574.

- [43] Farzaneh M & Chisholm W.A. *Insulators for icing and polluted environments*, IEEE Press series on Power Engineering, IEEE/John Wiley, New York, 2009.
- [44] Crocombette, C., *The weather impact on the transmission of electricity in France*. In: Proceedings of the 8th European Conference on Application of Meteorology, ECEAM07,2007.
- [45] DeGaetano, T., Belcher, B.N., Spier, P.L., *Short-term ice accretion forecasts for electric utilities using the weather research and forecasting model and a modified precipitation-type algorithm*. Weather Forecast. 23 (5), 838–853, 2008.
- [46] Yang Lin, Hao Yanpeng, Li Weiguo, et., *A mechanical calculation model for on-line icing-monitoring system of overhead transmission lines*. Proceeding of the CSEE, 2010.
- [47] Yu, Q., M. C. Zhou, and Z. Luo, *On-line robust identification of tool-wear via multi-sensor neural network fusion*, Engineering Application of Artificial Intelligence, 11, 717-722, 1998.
- [48] X.Feng, X. Kong, and H. Ma, *Coupled Cross-correlation Neural Network Algorithm for Principal Singular Triplet Extraction of a Cross-covariance Matrix*, IEEE/CAA Journal of Automatica Sinica, 3(2), 147-156, 2016
- [49] M. Yue, L. Wang, and T. Ma, *Neural network based terminal sliding mode control for WMRs affected by an augmented ground friction with slippage effect*, IEEE/CAA Journal of Automatica Sinica, 4(3), 498-506, 2017
- [50] H. J. Yang and J. K. Liu, *An adaptive RBF neural network control method for a class of nonlinear systems*, IEEE/CAA J. of Autom. Sinica, vol. 5, no. 2, pp. 457-462, Mar. 2018.
- [51] S. Li, M. Zhou, and X. Luo, *Modified Primal-Dual Neural Networks for Motion Control of Redundant Manipulators with Dynamic Rejection of Harmonic Noises*, IEEE Transactions on Neural Networks and Learning Systems, 29(10), pp. 4791 - 4801, Oct. 2018.
- [52] S. Gao, M. Zhou, Y. Wang, J. Cheng, H. Yachi, and J. Wang, *Dendritic neuron model with effective learning algorithms for classification, approximation and prediction*, IEEE Transactions on Neural Networks and Learning Systems, DOI: 10.1109/TNNLS.2018.2846646, on line, 2018.